AN INVESTIGATION OF SHEET-STIFFENER PANELS SUBJECTED TO COMPRESSION LOADS WITH PARTICULAR REFERENCE TO TORSIONALLY WEAK STIFFENERS

Thesis

by

Louis G. Dunn

In Partial Fulfillment of the Requirements for

the Degree of Doctor of Philosophy

California Institute of Technology

Pasadena, California

1940

SUMMARY

A total of 183 panel specimens of 24ST aluminum alloy with nominal thicknesses of 0.020, 0.025, and 0.040 inch with extruded bulb-angle sections of 12 shapes spaced 4 and 5 inches as stiffeners were tested to obtain the buckling stress and the amplitude of the maximum wave when buckled. Bulb angles from 3 to 27-1/2 inches long were tested as pin-end columns. The experimental data are presented as stress-strain and column curves and in tabular form. Some comparisons with theoretical results are presented.

Analytical methods are developed that make it possible for the designer to predict with reasonable accuracy the buckling stress and the maximum-wave amplitude of the sheet in stiffened-panel combinations. The scope of the tests was insufficient to formulate general design criteria but the results are presented as a guide for design and an indication of the type of theoretical and experimental work needed.

INTRODUCTION

This report presents the results of an investigation on the behavior of sheet-stiffener panels subjected to end compression.

In part I methods are developed for calculating:

(1) The buckling stress of a plate in which the edges parallel to the applied end load are elastically supported and the other two sides are simply supported. The elastic edge support corresponds to the restraining moments induced by the stiffener on the buckling of the sheet.

(2) The maximum-wave amplitude of the buckled sheet as a function of the stiffener stress and the buckling stress of the sheet.

A short discussion is also given in appendix A of the preliminary work done on the theoretical calculation of the stiffener stresses. Further necessary refinements in the theory are pointed out.

Part II consists of the experimental results obtained by testing a large number of panels in which the stiffeners were bulb angles of the type commonly used in aircraft construction. The effective width as a function of the stiffener stress was determined for panels with stiffeners of various cross sections and torsional rigidities. The effect of panel length on the failing stress of the stiffeners, the type of failure, and the panel deformations were also determined.

A method of determining the buckling stress of the sheet between stiffeners, by measuring the maximum-wave amplitude, is

given in appendix B.

The author wishes to express his thanks to the National Advisory Committee for Aeronautics for the grant under which this project was carried out.

He also wishes to acknowledge his sincere appreciation for the advice given by Dr. Th. von Karman and Dr. E. E. Sechler during the carrying out of the research program and to thank Mr. Hsue-Shen Tsien for numerous helpful suggestions, Mr. Walter B. Powell for his assistance in reducing test data, and the other members of the teaching staff for many excellent suggestions.

The stiffener sections used in the tests were provided through the courtesy of the Douglas Aircraft Company. The North American Aviation Company assisted by constructing the test panels.

I. THEORETICAL DISCUSSION OF THE PROBLEM

The stability of torsionally weak columns subjected to a compression load has been investigated by many scientists and the results are published in references 1 to 5. It is pointed out in reference 4 that the buckling of centrally loaded open-section columns will, in general, be accompanied by twisting of the cross section. The critical stresses and the axes of rotation, which are functions of the geometry of the column cross section, are discussed in detail. It is further shown that, as the slenderness ratio L/ρ of the column increases, the effect of twisting tends to be neutralized until finally the buckling is free from twisting and failure occurs by buckling as an Euler column.

The type of failure that occurs when an open-section column acting as a stiffener is attached to a thin sheet is essentially of the same type. It differs only in the respect that failure is not necessarily a stability phenomenon, even for lengths in which the column alone would fail owing to instability. A careful investigation of the twisting phenomenon in stiffened panels indicates that a gradual twisting of the stiffener occurs with increasing load until near the failing load, when the buckling rapidly increases and causes failure of the panel. The degree of twisting of the stiffener during loading of the panel depends on the torsional rigidity of the stiffener and on the thickness of the sheet to which the stiffener is attached.

The effect of the sheet on the stiffener may be summarized as follows:

(1) When the sheet buckles, the stiffener exerts a restraining moment on the sheet or, conversely, the sheet imparts to the stiffener a twisting moment that is proportional to the curvature of the sheet. In the analysis of isolated columns, this interaction of stiffener and sheet changes the homogeneous problem of torsional stability to a nonhomogeneous problem of gradual twisting for the case of open-section stiffeners attached to sheet. For torsionally weak stiffeners, it is important that the interaction of sheet and stiffener be taken into consideration.

(2) A column that fails by twisting will generally twist about an axis through its shear center. Owing to

the rigidity of the sheet in its own plane, however, the axis about which the column twists when attached to the sheet will not necessarily be the shear center of the column. If the column were to twist about some axis outside the plane of the sheet, a geometrical consideration shows that not only must the sheet move out of its own plane but the point of attachment must have a component of displacement parallel to the sheet, which is physically impossible. It seems logical to assume that the sheet will tend to shift the axis of twist toward the point of attachment of column and sheet. Although the point of attachment is geometrically the most natural position for the axis of twist, it cannot be concluded that the axis of twist will be at this point. No simple criterion can be given for the position of the axis of twist. Each different type of column, when attached to the sheet, must be considered as an individual problem. An extensive discussion regarding the axis of twist is given in reference 1.

(3) In certain cases, the axis of least radius of gyration of the stiffener will either be perpendicular to or be inclined to the plane of the sheet. In such cases, the sheet, owing to the rigidity in its own plane, will prevent column failure for lengths in which the stiffener alone would fail as an Euler column.

The Mutual Effects of Sheet and Stiffener

From the previous discussion it is evident that, for a theoretical treatment of the critical stresses in a stiffened panel, the following factors should be investigated:

(1) The influence of the stiffener on the elastic stability of the sheet; the type of wave form of the buckled sheet; and, as a consequence, the stress distribution in the sheet.

(2) The influence of the buckled sheet on the stiffener, especially near the stability limit of the stiffener.

From a consideration of a cross section of the panel with the sheet buckled, as shown in figure 1(b), it can be seen that, if the sheet is to assume the wave form as indicated, the stiffener must twist. If the stiffener makes a line rather than an area contact with the sheet, however, the sheet may assume the wave form as indicated

without appreciable twisting of the stiffener. It may therefore be concluded that, for the case in which the sheet is riveted at reasonably close intervals to a stiffener of the type shown in figure 1, the torsional rigidity of the stiffener will determine the amount of edge support of the sheet.

Stability of the Sheet between Stiffeners

The stability of a rectangular plate with elastic supports of finite torsional rigidity along two edges and with an axially applied load will be investigated under the following explicit simplifying assumptions:

(1) The sheet reaches its stability limit before any bending of the stiffener takes place. This assumption is reasonable for the type of stiffened panels used in aircraft construction.

(2) In order to eliminate secondary phenomena of instability in the stiffener region, it will be assumed that the center of twist of the stiffener is at the edge of the sheet and, furthermore, that the stiffener is concentrated at the edge of the sheet

(3) The material is homogeneous, isotropic, and obeys Hooke's law of deformation.

The general case, in which bending of the stiffener is considered, has been investigated by E. Chwalla (reference 6). The boundary conditions are, of necessity, rather complicated and the final solution is consequently too involved for general practical application.

The boundary conditions for the simplified case under consideration, with dimensions and loading as indicated in figure 2, are as follows:

At $x = 0$, $x = a$

$$w = 0 \tag{1}$$

$$\frac{\partial^2 w}{\partial x^2} + \nu \frac{\partial^2 w}{\partial y^2} = 0 \tag{2}$$

The boundary conditions are satisfied if the deflection

surface is represented by the expression:

$$w = f(y) \sin \frac{\pi x}{\lambda} \tag{3}$$

where $f(y)$ is a function of y only, and λ corresponds to a half-wave length, i.e., a/m.

At $y = \pm b/2$

$$w = 0 \tag{4}$$

A second boundary condition at the stiffener can be obtained as follows (reference 7, p. 343): The bending moments that appear along the stiffener during buckling are proportional at each point to the angle of rotation of the edge. The angle of rotation of the stiffener during buckling of the skin is equal to $\partial w/\partial y$ and the rate of change of this angle is $\partial^2 w/\partial y^2$. The twisting moment at any cross section of the stiffener in a direction of the x-axis is then:

$$T = C \frac{\partial^2 w}{\partial y^2}$$

where C is the torsional rigidity of the stiffener.

The rate of change of the twisting moment is numerically equal to the bending moment per unit length of the sheet along the stiffeners, or:

$$D\left(\frac{\partial^2 w}{\partial y^2} + \nu \frac{\partial^2 w}{\partial x^2}\right) = C \frac{\partial^3 w}{\partial x^2 \partial y} \quad \text{at} \quad y = b/2 \tag{5a}$$

$$-D\left(\frac{\partial^2 w}{\partial y^2} + \nu \frac{\partial^2 w}{\partial x^2}\right) = C \frac{\partial^3 w}{\partial x^2 \partial y} \quad \text{at} \quad y = -b/2 \tag{5b}$$

The boundary conditions at $y = b/2$ are not independent of those at $y = -b/2$. In equations (5a) and (5b),

D is the bending stiffness of the sheet $\left[\frac{Et^3}{12(1 - \nu^2)}\right]$

and ν is Poisson's ratio.

Using the relation for w as given by equation (3), one obtains:

$$\frac{\partial^2 w}{\partial y^2} = \sin \frac{\pi x}{\lambda} \frac{\partial^2 f(y)}{\partial y^2}$$

$$\frac{\partial^2 w}{\partial x^2} = - \frac{\pi^2}{\lambda^2} f(y) \sin \frac{\pi x}{\lambda}$$

$$\frac{\partial^3 w}{\partial x^2 \partial y} = - \frac{\pi^2}{\lambda^2} \sin \frac{\pi x}{\lambda} \frac{\partial f(y)}{\partial y}$$

Substitution in equation (5a) gives:

$$D \left[\sin \frac{\pi x}{\lambda} \frac{\partial^2 f(y)}{\partial y^2} - \frac{\nu \pi^2}{\lambda^2} f(y) \sin \frac{\pi x}{\lambda} \right] = - C \frac{\pi^2}{\lambda^2} \sin \frac{\pi x}{\lambda} \frac{\partial f(y)}{\partial y}$$

since $w = 0$ at $y = b/2$. The foregoing equation can be written in the form:

$$D \left. \frac{\partial^2 w}{\partial y^2} \right|_{y=b/2} = - C \frac{\pi^2}{\lambda^2} \left. \frac{\partial w}{\partial y} \right|_{y=b/2} \tag{6}$$

which is the second boundary condition at $y = b/2$.

It has been shown (reference 7, p. 338) that, if a rectangular sheet is elastically supported along the two edges $y = \pm b/2$, a general solution of the differential equation for the deflected sheet can be represented in the form:

$$f(y) = C_1 e^{-\alpha y} + C_2 e^{\alpha y} + C_3 \cos \beta y + C_4 \sin \beta y$$

where

$$\alpha = \sqrt{\frac{\pi^2}{\lambda^2} + \sqrt{\frac{\pi^2 \sigma t}{\lambda^2 D}}}$$

$$\beta = \sqrt{\frac{-\pi^2}{\lambda^2} + \sqrt{\frac{\pi^2 \sigma t}{\lambda^2 D}}}$$

and σ is the unit axial compressive stress in the sheet of thickness t.

If a condition of symmetry is assumed along the x-axis, the boundary conditions (4) and (6) can be satisfied by taking $f(y)$ as an even function of y, or:

$$f(y) = A \cosh \alpha y + B \cos \beta y \tag{7}$$

and

$$w = (A \cosh \alpha y + B \cos \beta y) \sin \frac{\pi x}{\lambda} \tag{8}$$

From the boundary conditions (4) and (6), the following two equations are obtained:

$$A \cosh \alpha \frac{b}{2} + B \cos \beta \frac{b}{2} = 0 \tag{9}$$

$$A \left(D\alpha^2 \cosh \alpha \frac{b}{2} + C \frac{\pi^2}{\lambda^2} \alpha \sinh \alpha \frac{b}{2} \right) -$$

$$- B \left(C \frac{\pi^2}{\lambda^2} \beta \sin \beta \frac{b}{2} - D\beta^2 \cos \beta \frac{b}{2} \right) = 0 \tag{10}$$

A limit $\sigma = \sigma_c$ of the elastic stability is reached when computations (9) and (10) yield for A and B a solution different from zero or when, in other words, the determinant of the coefficients of the system vanishes, i.e.,

$$-C \frac{\pi^2}{\lambda^2} \beta \sin \beta \frac{b}{2} \cosh \frac{b}{2} - D \beta^2 \cos \beta \frac{b}{2} \cosh \alpha \frac{b}{2}$$

$$-D \alpha^2 \cosh \alpha \frac{b}{2} \cos \beta \frac{b}{2} - C \frac{\pi^2}{\lambda^2} \alpha \sinh \alpha \frac{b}{2} \cos \beta \frac{b}{2} = 0 \tag{11}$$

Division by $\cosh \alpha \frac{b}{2} \cos \beta \frac{b}{2}$ gives:

$$C \frac{\pi^2}{\lambda^2} \beta \tan \beta \frac{b}{2} + D \beta^2 + D \alpha^2 + C \frac{\pi^2}{\lambda^2} \alpha \tanh \alpha \frac{b}{2} = 0$$

Combining terms and simplifying,

$$\beta \tan \beta \frac{b}{2} + \alpha \tanh \alpha \frac{b}{2} + \frac{2\lambda D}{\pi C} \sqrt{\frac{\sigma_c t}{D}} = 0 \tag{12}$$

Now

$$\alpha b = \sqrt{\frac{b^2\pi^2}{\lambda^2} + \sqrt{\frac{b^4\pi^2\sigma_c t}{\lambda^2 D}}}$$

Let $\frac{b^2}{\lambda^2}\pi^2 = \theta^2$ and $\frac{\sigma_c t b^2}{D} = \psi^2$

Then $\alpha b = \sqrt{\theta^2 + \theta\psi}$ and $\beta b = \sqrt{\theta\psi - \theta^2}$

Equation (12) can then be written in the form:

$$\sqrt{\theta\psi - \theta^2} \tan \tfrac{1}{2}\sqrt{\theta\psi - \theta^2} + \sqrt{\theta^2 + \theta\psi} \tanh \tfrac{1}{2}\sqrt{\theta^2 + \theta\psi} + \frac{2\lambda D\psi}{C\pi} = 0 \qquad (13)$$

Now $\frac{2\lambda D}{C\pi} = 2\frac{bD}{C}\frac{\lambda}{\pi b} = 2\frac{bD}{C}\frac{1}{\theta}$

Putting $\frac{bD}{C} = \mu$, equation (13) becomes:

$$\sqrt{\theta\psi - \theta^2} \tan \tfrac{1}{2}\sqrt{\theta\psi - \theta^2} + \sqrt{\theta^2 + \theta\psi} \tanh \tfrac{1}{2}\sqrt{\theta^2 + \theta\psi} + \frac{2\psi\mu}{\theta} = 0 \qquad (14)$$

The parameters involved may also be defined in physical terms as follows:

$\frac{\psi^2}{4\pi^2}$, ratio of critical stress at buckling to buckling stress in a long plate with simply supported edges.

π/θ, aspect ratio of buckled lobe (length in direction of loading divided by stiffener spacing).

μ, ratio of flexural rigidity of sheet panel between stiffeners to torsional rigidity of stiffener.

The parameter μ gives the influence of the ratio of the bending stiffness of the sheet to the torsional rigidity

of the stiffener on the critical buckling stress of the sheet.

It can be shown that equation (14) is identical with a special case of the general solution given in reference 6, for which it is assumed that $EI_{st} = A_{st} = \infty$ and C is finite, where EI_{st} is the bending stiffness of the stiffener and A_{st} is the area of the stiffener.

Since ψ, or in turn σ_c, is given by the transcendental equation (11) as a function of θ and ψ, it would be desirable to present the solution in graphical form, which would greatly facilitate the application to practical problems.

The graphical solution can be obtained in the following manner:

(1) Assume a constant value ψ and obtain the corresponding value of μ for various values of θ.

(2) Plot a family of curves with μ as a function of θ, ψ being constant for each curve.

Since θ is a function of the dimensions of the sheet, a cross plot of ψ against a/b can be obtained for constant values of μ. From these cross plots, the value of σ_c, the buckling stress of the sheet, can be obtained if the value of C is known, because all other quantities will consist of the known dimensions and properties of the sheet.

The torsional stiffness C of the stiffener can be experimentally determined or can be calculated by the method given on page 257 of reference 8.

The graphical solution in which ψ is plotted as a function of a/b for constant values of μ is shown in figure 3.

The theory has been developed for a plate elastically supported along two edges. If a continuous sheet and stiffener panel is considered, the sheet on each side of the stiffener will transmit bending moments to the stiffener. It can be shown that, for symmetrical buckling, these moments will have the same sense. From these considerations it is evident that, for a continuous sheet, the effective

torsional rigidity will be one-half of that used in the graphical solution as given in figure 3. This fact must be kept in mind in the calculation of μ.

The validity of the solution was experimentally checked with a test panel designed to have a value of $\mu = 4.80$. The buckling load was obtained by measuring the maximum amplitudes for various increments of load. The amplitude was plotted as a function of the applied load and the buckling stress of the sheet was obtained by the method illustrated in appendix B. The theoretically calculated buckling load was 11 percent lower than the experimental value. A similar check was made on panels with 0.040-inch sheet and bulb angle 10265 as stiffeners. The theoretical value in this case was 7 percent lower than the experimental value. A detailed discussion of the panel properties is given in appendix B.

Influence of the Sheet on the Stiffener

The problem treated in the previous section of this report is of the classical type of stability problems. The influence of the sheet on the stability of the stiffener is a much more complex problem. Since, in general, the sheet buckles much sooner than the stiffener, it is necessary to consider the stress distribution of the sheet in the buckled state. This distribution cannot be determined without taking into account finite deformations.

It is evident from equation (5) that increments of torsional moments proportional to the curvature of the sheet are induced on the stiffener by the sheet. The magnitude of these torsional moments will depend upon the dimensions and the physical properties of the sheet, which, in general, will be known quantities, and on the wave form and the amplitude of the waves. In order to determine the magnitude of the torsional moments, the amplitude and the wave form must be known.

The author and the members of the group for structural research at GALCIT (Guggenheim Aeronautics Laboratory of the California Institute of Technology) are working on a theory suggested by the experimental work of this report that presumably will result in the determination of the wave form as a function of the load. In the present report, the problem is treated under the following simplifying assumptions:

(1) After buckling, the average stress in the sheet at the median fiber along the line $y = 0$ (fig. 2) is assumed to remain constant and equal to σ_c, the buckling stress of the sheet. It should be clearly understood that the assumption of constant stress is used only in those subsequent calculations involving the axial deformation of a sheet element, at $y = 0$, due to the external load. The local stress, at the median fiber, will actually be a variable over the length of the panel because buckling of the sheet causes induced stresses. The magnitude of these induced stresses will depend upon the boundary conditions of the problem. The change in the average stress along the line $y = 0$ after buckling will, in general, be small compared with the change in the edge stress, i.e., at $y = b/2$. According to equation (17) (given later), the maximum amplitude is a function of $\sqrt{\epsilon_{st} - \epsilon_c}$, where ϵ_{st} is the average unit strain along the lines $y = b/2$ and ϵ_c is the average unit strain along the line $y = 0$. A comparison between calculations based on the experimental observations given in figures 20 and 21 of reference 9 and those based on the assumption that ϵ_c = constant is shown in figure 4, in which $\sqrt{\epsilon_{st} - \epsilon_c}$ is plotted as a function of ϵ_{st}. The average strain along the line $y = 0$ was obtained from figure 21 of reference 9 and the average strain along $y = b/2$ from figure 20 of reference 9. The unit strain at buckling was estimated from the experimental observations to be 2.2×10^{-4}. The results shown in figure 4 indicate that, assuming no experimental error, the maximum error involved in the amplitude calculation based on the assumption that ϵ_c = constant is of the order of 5 percent.

(2) As a first approximation, it will be assumed that the wave form after buckling is the same as that at the stability limit.

Before the interaction between the buckled sheet and the stiffener is calculated, the maximum deflections of the sheet are calculated according to assumptions (1) and (2) and compared with the experimental evidence.

For the case of symmetry, the maximum amplitude will occur at the point $y = 0$, $x = \lambda/2$ and will be calculated according to the foregoing assumptions. An element of thin sheet subjected to an axial compressive load will deform

in the axial direction an amount proportional to $\sigma L/E$ until buckling takes place. Beyond the buckling load, the deformation will be a function of the axial compressive stress in the sheet and the magnitude of the compression waves.

Let ξ_T be the total deformation in the x-direction.

ξ_c, deformation due to axial compressive stress.

ξ_s, deformation due to wave formation.

Then
$$\xi_T = \xi_c + \xi_s \tag{15}$$

where
$$\xi_c = \frac{\sigma_c a}{E_s}$$

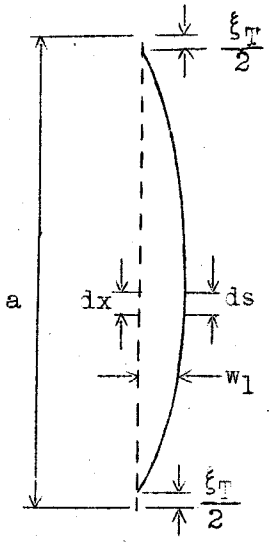

If ds is the length of an element of buckled sheet and the corresponding element of chord is dx, then the displacement due to bending is:

$$d\xi_s = ds - dx = \sqrt{dx^2 + dw_1^2} - dx$$

from which

$$d\xi_s = dx \sqrt{1 + \left(\frac{dw_1}{dx}\right)^2} - dx$$

Assuming dw_1/dx small and expanding gives:

$$d\xi_s = \frac{1}{2}\left(\frac{dw_1}{dx}\right)^2 dx$$

$$\xi_s = \frac{1}{2}\int_0^a \left(\frac{dw_1}{dx}\right)^2 dx$$

For the case in which the stiffener is not buckled $\xi_T = \frac{\sigma_{st} a}{E_{st}}$. Substituting in equation (15):

$$\frac{\sigma_{st}}{E_{st}}a = \frac{\sigma_o}{E_s}a + \frac{1}{2}\int_o^a \left(\frac{dw_1}{dx}\right)^2 dx \qquad (16)$$

where σ_c is buckling stress in sheet.

σ_{st}, axial compressive stress in stiffener.

E_s, Young's modulus for sheet.

E_{st}, Young's modulus for stiffener.

According to the stated assumptions, along the line $y = 0$, the deflected surface is given by:

$$w_1 = f_o \sin \frac{\pi x}{\lambda}$$

where f_o is the amplitude at $y = 0$, $x = \lambda/2$, from which

$$\frac{1}{2}\int_o^a \left(\frac{dw_1}{dx}\right)^2 dx = f_o^2 \frac{\pi^2}{2\lambda^2}\int_o^a \cos^2 \frac{\pi x}{\lambda} dx = \frac{a\pi^2}{4\lambda^2} f_o^2$$

Substituting in equation (16) and solving for f_o/λ gives:

$$\frac{f_o}{\lambda} = \frac{2}{\pi}\sqrt{\frac{\sigma_{st}}{E_{st}} - \frac{\sigma_c}{E_s}}$$

The preceding equation may be written in the form:

$$\frac{f_o}{\lambda} = \frac{2}{\pi}\sqrt{\epsilon_{st} - \epsilon_c} \qquad (17)$$

where ϵ_{st} is the unit deformation of the stiffener (σ_{st}/E_{st}) and ϵ_c is the unit deformation of the sheet at buckling (σ_c/E_c). Beyond the proportional limit, the value of ϵ_{st} should be determined from the stress-strain curve of the stiffener. The value of σ_c is obtained from the curves of figure 3. Values of f_o/λ for stiffener stresses up to 27,000 pounds per square inch have been obtained by experimental methods. The curve of f_o/λ

against $\sigma_{st} - \sigma_c$ in figure 5, obtained from equation (17), indicates a remarkably good agreement with the experimental results.

II. EXPERIMENTAL TECHNIQUE AND RESULTS

The extensive use of extruded sections as reinforcing members in metal-aircraft construction makes it desirable to investigate the behavior under load of such sections when attached to thin sheet. A systematic study of the behavior of bulb angles under load, as columns and as reinforcing members in thin sheet-metal construction, was undertaken at the California Institute of Technology during the school year 1936-37. During the first year, a series of tests was conducted to determine the ultimate strength of different bulb angles as pin-end columns and of panels in which one of these bulb angles (10282) was used as a stiffener. This part of the investigation was carried out by Lieutenant (J.G.) Joseph N. Murphy, U.S.N., and Captain Joe N. Smith, U.S.M.C. The investigation has been continued by the author.

The analytical investigation carried on as a part of the study indicated the desirability of a more thorough testing procedure. Consequently, in addition to determining the ultimate load of the panel, stiffener deformations were measured at intermediate loads and records were made of the wave pattern of the buckled sheet. Knowing the stiffener deformation for a given load, a curve of average stress as a function of stiffener strain could be plotted. It was then possible, with the aid of the stress-strain diagram of the stiffener alone, to determine that portion of the total load carried by either the stiffeners or the sheet throughout the entire range of load. From these data, the effective width of the sheet acting with the stiffeners at any stiffener stress could be calculated and plotted.

Column curves of the average stress at failure were plotted as a function of the effective slenderness ratio of the panels. These curves indicated the effect of the column length on the ultimate stresses.

The wave-pattern records were used to check the theoretically calculated values of the buckling stress and the maximum-wave amplitude of the sheet.

The theoretical analysis also indicated that a knowledge of the torsional rigidity of the stiffeners was required. The torsional rigidity of bulb-angle sections being rather difficult to calculate, this property was experimentally determined.

Materials

The extruded bulb-angle sections used in the tests were fabricated from 24ST aluminum alloy. (See fig. 6.) The sheet was also of 24ST alloy with a nominal thickness of 0.020, 0.025, and 0.040 inch. The strength properties of five of the bulb-angle sections are given in figure 7 and table I.

Test Specimens

The panel lengths were so chosen as to cover the complete range of bulkhead spacings that might be encountered in current aircraft design practice and were such as to cover the normal short-column range and, in certain instances, depending on the dimensions of the bulb angle, were such as to reach the long-column range.

The number of stiffeners was varied in order to investigate the effect, if any, of the number of stiffeners on the ultimate stiffener stresses.

A typical example of one of the 183 panel specimens is shown in figures 8 and 9. The dimensions of the specimens and the test data are given in tables II to VII. For panels 148 to 183, the stiffener spacing was 4 inches. On all other panels, the spacing was 5 inches. The rivet spacing, which was three-fourths inch in all cases, was chosen so that premature buckling of the sheet between rivets would not occur for either the thin or the thick sheet. On each panel, the sheet extended beyond the outboard stiffener a distance equal to half the stiffener spacing.

In order to obtain square and parallel ends, all panels were carefully milled in a milling machine, the ends being kept parallel to within 1/1000 inch.

After completion of the tests of panels 130 to 138, check panels were tested to minimize the experimental scatter.

Bulb angles from 3 to 27½ inches in length were tested as pin-end columns, this variation in length being sufficient to cover both the short-column and the long-column ranges. Cross sections of the test specimens are shown in figure 6. Stiffener columns 2½ inches in length were tested flat-ended to obtain a compression stress-strain curve for each of the bulb-angle sections used in panels 1 to 130. Specimens 15 to 20 inches in length of this last group of stiffeners were also tested in torsion.

Owing to manufacturing tolerances, the dimensions of the specimens varied considerably from the specifications. In particular, the bulb angles were subject to at least an 8-percent variation in cross-sectional area. The dimensions shown in figure 6 are the nominal dimensions. All specimens were checked with a micrometer caliper, and the actual dimensions were used in reducing the test data.

Test Apparatus and Testing Procedure

All panel specimens were tested flat-ended in a standard 150,000-pound Olsen testing machine. (See fig. 10.) The column tests were conducted in a 3,000- and a 30,000-pound Riehle testing machine, and the torsion tests in a small torsion machine built by the Scientific Instrument Company.

Two special face plates were made to insure an even load distribution over the panel. Their surfaces were kept parallel to within 1/1000 inch. The two face plates were placed between the heads of the testing machine and the test panel was mounted between them. A small load was applied to hold the panel in place while Huggenberger tensiometers were mounted on each stiffener as shown in figure 10. The tensiometers were in all cases mounted as near as possible to the centroid of the bulb angle.

The free edges of the panels were supported by slotted steel tubes, 3/4-inch outside diameter by 0.093 inch, a clearance of approximately 1/8 inch being allowed at each end of the panel. It was felt that clamping the tubes to the sheet would give too great a rigidity to the free edges; hence, the edges were merely inserted in the slot, which was such as to give a sliding fit over the sheet. This condition would probably closely approximate a condition of simple support, the effect of which can be calculated.

When the load was applied, notwithstanding the care exercised in milling the ends of the test panel and in using the face plates, the load distribution over the width of the panel was found to be uneven. This unevenness was due to nonparallel motion of the movable head of the testing machine with reference to the fixed base and necessitated shimming the face plates until the tensiometer readings indicated an even load distribution.

A special machine consisting essentially of a carriage that moved along a vertical column was designed to trace and record the wave form of the buckled sheet. (See fig. 11.) A rack with a roller on one end projects from the carriage to the panel, so that the end of the rack can follow the contour of the waves. This rack, through a suitable amplifying gear train, operates a pen that traces the profile of the wave on one face of an octagonal recording drum. The gear sizes are so chosen as to give a 1:5 amplification on the record. A light spring is used to load the device and keep the roller on the first rack always in contact with the sheet. The vertical column can be moved transversely, permitting an axial trace of the wave amplitude to be made at any place on the sheet.

After the initial load had been applied and the tensiometers placed on the stiffeners, the loading was increased in 12 to 15 increments until failure occurred. Just before failure, the tensiometers were removed. Tensiometer readings were taken for each increment of load, and tracings of the wave profile at various places on the panel were made several times in the course of the test. A few of the panels were tested without instruments, only the failing load being recorded.

The ends of the stiffener specimens tested in torsion alone were cast, by means of Wood's metal, into oversize sockets that fitted into the torsion machine. This set-up is shown in figure 12. It was thus possible to aline the shear center of the bulb angles with the axis of the machine.

Experimental Data

Calculation of effective width from experimental data.- The effective width of a stiffened panel can be calculated for any given load if the stiffener stress is known. The stiffener stress up to the proportional limit can be directly obtained from the tensiometer readings by means of the

equation

$$\sigma_{st} = k\ R\ E \tag{18}$$

where σ_{st} is the stiffener stress, pounds per square inch.

k, tensiometer constant.

R, tensiometer reading.

E, Young's modulus.

In order to obtain the stiffener stress beyond the proportional limit, flat-end compression tests were conducted on $2\frac{1}{2}$-inch specimens. The stress-strain curves for five of the bulb angles used as stiffeners are shown in figure 7. Using the strain reading for the panel, the corresponding stress could be obtained from the stress-strain curves. Where the stress-strain curves for the check specimens deviated, an average value was used. A tension stress-strain curve for specimen 8478 was plotted on the same figure to give a comparison of the strength properties of the specimen in tension and compression.

The load carried by the sheet is given by the equation:

$$P_s = P - n\ A_{st}\ \sigma_{st} \tag{19}$$

and the effective width acting with each stiffener by:

$$w_e = \frac{P_s}{2(n + k_1)t\ \sigma_{st}} = \frac{P - n\ A_{st}\ \sigma_{st}}{2(n + k_1)t\ \sigma_{st}} \tag{20}$$

where P is total applied load, pounds.

w_e, effective width of sheet acting with each stiffener (reference 10).

A_{st}, stiffener area, square inches.

n, number of stiffeners.

t, sheet thickness.

k_1, ratio between load carried by each effective width of sheet and additional load carried by outside sheet panels due to edge supports.

Evaluation of k_1.- The effect of the tube over the free edge of the panel is to stiffen the sheet between the stiffener and the tube; and, in effect, the panel width is 2.5 inches rather than 5 inches. Because the panel width is decreased, the critical buckling stress of the sheet is increased and the sheet between the tube and the stiffener will be acting at a higher average stress than the sheet between the two bulb angles. The effective width being proportional to the load carried by the sheet, the ratio of the additional load carried by the sheet to the load that would normally be carried if the panel were continuous can be given by the equation:

$$k_1 = \frac{w_{e_T} - w_e}{w_e} \tag{21}$$

where w_{e_T} is the effective width between tube and stiffener. The effect of the edge supports is illustrated in figure 13. No theory that gives a correct calculation of the effective width in a stiffened panel at present exists. The equation given on page 28 of reference 11 was considered to give the best approximation. Here Marguerre suggests the following equation (in the notation of the present paper) for values of $1 < \frac{\sigma_{st}}{\sigma_c} < 75$:

$$w_e = \frac{b}{2}\sqrt[3]{\sigma_c/\sigma_{st}} \tag{22}$$

where b is stiffener spacing, inches.

σ_c, critical buckling stress of sheet between stiffeners, pounds per square inch.

Assuming that the effective width due to the tube can be calculated in the same manner, and if

σ_c' is the critical buckling stress of sheet between stiffener and tube, pounds per square inch,

b', spacing between stiffener and tube,

then

$$w_{e_T} = b' \sqrt[3]{\sigma_c'/\sigma_{st}} \tag{23}$$

Noting that in this case $b/2 = b'$ and substituting equations (22) and (23) in (21) gives:

$$k_1 = \sqrt[3]{\sigma_c'/\sigma_c} - 1 \tag{24}$$

It should be noted that, for all values of $\sigma_{st} \leq \sigma_c$, $k_1 = 0$ since $\sigma_c = \sigma_c' = \sigma_{st}$ and, for all values of $\sigma_{st} \geq \sigma_c$, $k_1 =$ constant.

The buckling stress, σ_c, can be computed by means of the curves given in figure 3, if the torsional rigidity of the stiffener is known. As a first approximation, σ_c' was evaluated in the following manner:

(a) Calculate the buckling stress of the sheet, between the stiffener and the tube, assuming the conditions of support at the tube to be the same as those at the stiffener.

(b) Calculate the buckling stress assuming simple support at both stiffener and tube.

The value of σ_c' was then assumed to be the average of the two calculated buckling stresses.

A plot of k_1 as a function of stiffener stress, for the various sheet and stiffener combinations, is shown in figure 14. Knowing the value of k_1 as a function of the stiffener stress, the average effective width was calculated by means of equation (3). The stiffener area and the skin thickness used in these calculations were computed from the measured dimensions of each stiffener. The stiffener stress σ_{st} and the total load P can be obtained from the curves (figs. 15 to 25) of average stress plotted against stiffener strain. By average stress is meant the applied load divided by the total cross-sectional area of the test panel. The strain against which the average stiffener stress is plotted is an average value of the measured strains for each stiffener.

The experimental values of w_e/b as a function of the stiffener stress are shown in figures 26 to 35. In or-

der to compare the experimental values with some of the existing theoretical work (references 10 to 13), the average values of w_e/b were plotted as a function of σ_{st}/σ_c and are shown in figure 36.

Maximum amplitude.- A record of the wave pattern was made along a line midway between the stiffeners to determine the maximum amplitude of the buckled sheet for a given load. From this tracing, the half-wave length and the maximum amplitude could then be determined. The points plotted in figure 5 correspond to the average value of f_o/λ taken over the entire length of the panel. The stiffener stress corresponding to the particular load for which the wave record was made was obtained from the measured stiffener deformations. The buckling stress σ_c was computed by the curves given in figure 3 using the minimum value of ψ.

Column curves.- Owing to the large stiffener deformations, the tensiometer readings became very irregular near the ultimate load. The readings near the failing load were therefore felt to be insufficiently accurate to define the ultimate stress of the stiffeners. For this reason, the average ultimate stress of the panels was used in plotting the column curves of the test results. The value of ρ, the effective radius of gyration of the sheet stiffener combination at failure, could be approximated by the following method.

Calculations were made to determine the value of ρ for the stiffener with various amounts of effective width. The change in ρ for these combinations was found to be quite small within the range of effective width in which failure was assumed to occur. It was possible to determine closely the values of L/ρ for the panels at failure, even though the corresponding value of stiffener stress was quite uncertain. Column curves showing the average stress at failure as a function of L/ρ could then be plotted for the various panels. The results are shown in figure 37.

Torsional rigidity of bulb angles.- Torsion tests were conducted on a number of the bulb-angle specimens used as stiffeners. In order to obtain a proper grip on the test specimens, the ends were cast into oversize sockets that fitted into the torsion machine. Care was taken to obtain a proper alinement with the shear center of the

bulb angle and the axis of rotation of the test machine. The ends were cast in Wood's metal and the tests therefore corresponded to torsion with end restraint.

The applied torsional moment of five stiffeners is plotted against the corresponding torsional deflection in figure 38. The torsional rigidity of the stiffener was calculated from the equation

$$C = M_T/\varphi$$

where M_T is the torsional moment, inch-pounds.

φ, torsional deflection, radians per inch.

Column curve of stiffeners alone.- The experimental data of the stiffener tested as pin-end columns are given in table VIII; the results are plotted in figure 39.

Comparisons of the results with the "straight-line formula" and with the Johnson parabolic formula are indicated in figure 39. For values of $80 < L/\rho < 230$, the points scatter about the Euler curve; and, for values of $L/\rho < 80$, most of the test points scatter about the straight-line formula.

The test results of figures 37(c) and 39 were taken from the work done by Lieutenant (J.G.) Joseph N. Murphy, U.S.N., and Captain Joe N. Smith, U.S.M.C.

Discussion of Experimental Results

Effective width.- The average values of the measured effective width are plotted as a function of the dimensionless parameter σ_{st}/σ_c as shown in figure 36. These curves indicate a marked increase in effective width with an increase in the torsional rigidity of the stiffener. In general, the buckling stress, σ_c, of the sheet will depend on the torsional rigidity of the stiffener and the method of attaching the sheet to the stiffener. The value of σ_c was computed for each sheet-stiffener combination by the method illustrated in appendix B. In view of the reasonably close experimental check of the method, it is felt that the difference in the effective-width curves is due not to an error in σ_c but rather to a difference in wave form.

The restraining moment exerted by the stiffener on the sheet will, in general, affect the wave form of the buckled sheet. This restraining moment will vary with the stiffener stress and the stiffener cross section for it can be seen from equation (25) (appendix A) that the inclination of the stiffener is a function of the bending moment induced by the sheet, the stiffener stress, the torsional rigidity, and the torsion-bending constant of the stiffener.

The difference between the measured effective width and that calculated from existing theory is largely due to the fact that the influence of the stiffener on the buckled sheet has in no case been correctly considered. The edge effect of the stiffener has, in general, been assumed to be equivalent to a simple support, that is, no restraining moment along the stiffener. This assumption is incompatible with the required conditions of continuity of the sheet and stiffener inclination at the stiffener.

The measured effective width indicates a considerable drop near the ultimate stress of the stiffener. This drop can probably be accounted for by the fact that, near the failing load, the torsional deflection of the stiffener and the maximum amplitude of the buckled sheet will rapidly increase. The increase in amplitude is evident from equation (17), since the term ϵ_{st}, which is the unit deformation of the stiffener, will be nonlinear beyond the proportional limit of the stiffener. As the ultimate stress is approached, the deviation from a linear variation rapidly increases. The variation of torsional deflection with stiffener stress is indicated in figure 40.

No consistent variation of effective width could be detected with a change in panel length. The measured values show, in general, a random scatter about a mean curve.

Maximum amplitude.- For stiffener stresses up to 27,000 pounds per square inch, the measured maximum amplitude indicates a good agreement with the theoretical values calculated by equation (17). The curve shown in figure 5 is calculated for a linear variation of ϵ_{st}; hence, beyond the proportional limit of the stiffener, the curve will deviate from measured values.

Column curves.- Although the column curves shown in

figure 37 are not indicative of the true ultimate stiffener stress, the curves nevertheless do show the effect of panel length on the ultimate stress. The column curves in the range of $10 < L/\rho < 80$ indicate but a very small variation in stress, which is to be expected, since failure occurred by twisting of the stiffeners. In the case of twisting failure, the stiffener tends to rotate in the same direction as the buckled sheet. This result means that a section of the stiffener corresponding to a half-wave length of the buckled sheet tends to twist in one direction and an adjacent section of the same length twists in the opposite direction. This type of failure should not be affected to any appreciable extent by the length of the panel, provided that the length is such as to fall below the Euler range or above the half-wave length of the twisted column.

Bulb angles 8477 and 10266 failed by combined twisting and bending in the 21-inch and the 27-inch panels. This type of failure is characterized by a gradual twisting of the stiffener until a stress is reached at which the column fails by bending. Owing to the distortion of the stiffener by the twisting action, the section properties may change in such a manner that the slenderness ratio is effectively increased. A failure of this type may occur at a lower stress than the value given by the Euler formula, or for a pure twisting failure.

CONCLUSIONS

The primary purpose of the investigation was to obtain a better understanding of the behavior of stiffened panels such as are used in aircraft construction. The scope of the tests is insufficient for general design criteria, but the results should be of considerable value as a guide in design work and in future theoretical work on this problem.

Analytical methods that make it possible for the designer to predict with reasonable accuracy the buckling stress and the maximum-wave amplitude of the sheet in stiffened-panel combinations have been developed. It is felt that a complete theoretical treatment of the problem, although admittedly difficult, is not entirely impossible. Such an analysis would simplify the work of the designer and eliminate the need for many costly tests.

Guggenheim Aeronautics Laboratory,
California Institute of Technology,
Pasadena, Calif., April 1939.

APPENDIX A

Discussion of Stiffener Stresses

By the use of equation (17) as a boundary condition at $y = 0$ and the boundary condition that $w = 0$ at $y = \pm b/2$, the constants A and B of equation (7) can be evaluated. Under assumption (2), the moment transferred from the sheet to the stiffener can then be evaluated. From a consideration of equilibrium of the stiffener, the following differential equation giving the form of the strained column can be derived:

$$E C_{BT} \frac{d^4\varphi}{dx^4} + (\sigma_x I_p - C) \frac{d^2\varphi}{dx^2} - m_y = 0 \qquad (25)$$

where E is Young's modulus.

C_{BT}, torsion bending constant (references 1 to 5).

σ_x, axial compressive stress in stiffener.

I_p, polar moment of inertia about axis of twist.

C, torsional rigidity of stiffener.

m_y, moment transferred by buckled sheet to stiffener.

φ, torsional deflection of stiffener.

If the value of m_y is known and the end effects are neglected, the inclination φ can be calculated by means of equation (25). This value of φ can be compared with a value of φ calculated from the assumptions that:

(1) After buckling, $\sigma = \sigma_c$ = constant at $y = 0$.

(2) The wave form does not change.

In order to simplify the calculations, it was assumed that a stiffener as shown in figure 40 is attached to a sheet having a thickness of 0.040 inch. The stiffener spacing was assumed to be 5 inches and the axis of twist to be at the position indicated.

If the assumptions (1) and (2) are compatible with the stiffener properties, the two calculated slopes should coincide. From an examination of figure 40, it can be seen that a fairly good agreement is obtained for stiffener stresses up to 20,000 pounds per square inch. Beyond this value of σ_x, the deviation increases rapidly with an increase in σ_x. It may therefore be concluded that either assumption (1) or (2) or both are invalid, especially for high stiffener stresses. In view of the good agreement obtained for the theoretically calculated maximum amplitude and the experimental values, it is felt that assumption (2) is chiefly responsible for the discrepancy. A further refinement in the analysis is thus necessary and should be carried out.

It should be noted that equation (25) describes only the case in which failure takes place by twisting of the column. The experimental observations have indicated that, for panel lengths near or in the Euler range, the stiffener may fail by combined twisting and bending. This case is an important one because the critical stress will, in general, be lower than that given by either the Euler formula or by a formula derived for a pure twisting failure.

A theory that describes this type of failure as well as that for pure twisting should be of considerable importance in airplane design and therefore deserves an extensive investigation.

APPENDIX B

Experimental Check of the Theoretical Buckling Stress of the Sheet

It was desired to obtain an experimental verification of the theoretical calculations of the buckling stress of the sheet for different values of μ. Since μ was relatively small for all the bulb angles tested, it was necessary to design a panel having a larger value of μ; that is, a value that more closely approached a simply supported edge condition. A stiffened panel was designed in which the stiffeners consisted of bent-up angle sections, 0.051 by 3/4 by 3/4 inch, riveted to an 0.064-inch sheet. The panel was essentially of the same type as the bulb-angle panels with the exception that the angles were riv-

eted on each side of the panel, i.e., back to back. Three check panels designated panels A, B, and C of this design were tested and their dimensions and properties are given in table IX. Figure 41 shows test specimen A.

In order to determine the buckling stress, wave records were made midway between stiffeners at various load increments. From these wave records, it was possible to obtain f_o/λ. A convenient method of determining the buckling stress is to write the following functional relationship for P, the applied load, and f_o/λ.

Since P is independent of the direction in which the sheet buckles, write:

$$P = \text{even function of } f_o/\lambda$$

Then, by a Taylor's expansion,

$$P = P_o + \frac{P''}{2!}(f_o/\lambda)^2 + \frac{P''''}{4!}(f_o/\lambda)^4 + \cdots$$

Putting

$$(f_o/\lambda)^2 = u$$

write

$$P = P_o + A_1 u + B_1 u^2 + \cdots$$

If u is plotted as a function of P, the resulting curve will be very close to a straight line for small values of μ, and P_o will correspond to the buckling load.

The generality of the foregoing discussion is unaltered if P is divided by the cross-sectional area A of the panel. A plot of $(f_o/\lambda)^2$ as a function of P/A, for the panels described and for panels of 0.040-inch sheet with bulb angle 10265, is shown in figure 42. The buckling stresses indicated by these curves are 8,000 and 3,900 pounds per square inch, respectively.

The torsional rigidity of the angle section used in panels A, B, and C is, from figure 38,

$$C = M_T/\varphi = 250 \text{ pound-inches}^2$$

Since the sheet was stiffened by two angles, the torsional rigidity of the combination is 500 pound-inches^2.

Assuming $E = 10^7$ pounds per square inch, $\nu = 0.3$, then, for $b = 5$ inches and $a/b = 3.2$,

$$\mu = \frac{bD}{C} = \frac{bEt^3}{12(1 - \nu^2)C} = 2.4$$

As has been pointed out, only half of this value of C should be used for the case in which the sheet extends on both sides of the panel; hence, the effective value of μ is 4.8.

From the curves of figure 3, the value of ψ corresponding to $\mu = 4.8$ is 6.87. Hence

$$\sigma_c = \frac{\psi^2 Et^2}{12(1 - \nu^2)b^2} = 7,100 \text{ pounds per square inch}$$

For the 0.040-inch sheet and bulb angle 10265, the effective value of $\mu = 0.636$, the corresponding value of $\psi = 7.83$, and the buckling stress = 3,620 pounds per square inch.

It follows from the definition of ψ that the stiffness of the stiffeners has increased the buckling stress of the 0.064-inch sheet by 20 percent and the 0.040-inch sheet by 55.5 percent since

$$\left(\frac{\psi^2}{4\pi^2}\right)_{0.064} = 1.20$$

and

$$\left(\frac{\psi^2}{4\pi^2}\right)_{0.040} = 1.555$$

The calculated buckling stresses are, in both cases, lower than the given measured values. The discrepancy can be explained by the fact that, in the test panel, longitudinal warping of the end cross section of the stiffener is prevented, resulting in a nonuniform twist. In the case of nonuniform twisting, part of the torque is resisted by bending of the flanges and gives effectively a higher torsional rigidity of the stiffener.

It is felt that, in the described torsion experiments, longitudinal warping was only partly prevented. Hence, the torsion constants obtained from these tests would be lower than the values realized in the panel tests.

REFERENCES

1. Lundquist, Eugene E., and Fligg, Claude M.: A Theory for Primary Failure of Straight Centrally Loaded Columns. T.R. No. 582, N.A.C.A., 1937.

2. Wagner, Herbert: Torsion and Buckling of Open Sections. T.M. No. 807, N.A.C.A., 1936.

3. Wagner, H., and Pretschner, W.: Torsion and Buckling of Open Sections. T.M. No. 784, N.A.C.A., 1936.

4. Kappus, Robert: Twisting Failure of Centrally Loaded Open-Section Columns in the Elastic Range. T.M. No. 851, N.A.C.A., 1938.

5. Lundquist, Eugene E.: The Compressive Strength of Duralumin Columns of Equal Angle Section. T.N. No. 413, N.A.C.A., 1932.

6. Chwalla, E.: Das allgemeine Stabilitätsproblem der gedruckten, durch Randwinkel verstärkten Platte. Ing.-Archiv, VIII. Bd., 1. Heft, Feb. 1934, S. 54.

7. Timoshenko, S.: Theory of Elastic Stability. McGraw-Hill Book Co., Inc., 1936.

8. Timoshenko, S.: Theory of Elasticity. 1st ed., McGraw-Hill Book Co., Inc., 1934.

9. Ramberg, Walter, McPherson, Albert E., and Levy, Sam: Experimental Study of Deformation and of Effective Width in Axially Loaded Sheet-Stringer Panels. T.N. No. 684, N.A.C.A., 1939.

10. Sechler, E. E.: Stress Distribution in Stiffened Panels under Compression. Jour. Aero. Sci., vol. 4, no. 8, June 1937, pp. 320-323.

11. Marguerre, Karl: The Apparent Width of the Plate in Compression. T.M. No. 833, N.A.C.A., 1937.

12. von Kármán, Theodor, Sechler, Ernest E., and Donnell, L. H.: The Strength of Thin Plates in Compression. A.S.M.E. Trans., APM-54-5, vol. 54, no. 2, Jan. 30, 1932, pp. 53-57.

13. Cox, H. L.: The Buckling of Thin Plates in Compression. R. & M. No. 1554, British A.R.C., 1933.

TABLE I

Stiffener Properties

(Nominal dimensions used in calculations; strength properties obtained from 2-1/2-inch specimens)

Bulb angle	Area (sq.in.)	I_{xx} ($in.^4$)	I_{yy} ($in.^4$)	Young's modulus (kips/sq.in.)	Torsional rigidity (inch-pound / radians-inch)	Ultimate strength in compression (lb./sq.in.)
10265	0.0900	0.0094	0.00113	10380	919.6	39300
8478	.1680	.0281	.00877	10000	2332	38800
8477	.2669	.0398	.01627	10000	6500	42400
8476	.1483	.0474	.00333	10080	2045	42100
106	.0684	.00443	.00443	10480	250	30000

TABLE III

Panel Specimens with Bulb Angle 8477

Panel	Panel length (in.)	Sheet thickness (in.)	Bulb angle area (sq.in.)	Sheet area (sq.in.)	Total area (sq.in.)	Ultimate load (lb.)	Average stress σ_a (lb./sq.in.)	ρ	L/ρ
			3 stiffener panels; 0.025-inch sheet						
48	3.88	0.0242	0.7704	0.363	1.133	35250	31100	0.389	9.98
49	3.94	.0249	.7749	.373	1.148	35150	30630	.389	10.1
50	7.97	.0242	.7743	.363	1.137	34100	30000	.389	20.5
51	7.97	.0243	.7695	.364	1.134	34650	30550	.389	20.5
52	11.94	.0246	.7755	.369	1.145	34525	30120	.389	30.7
53	11.97	.0249	.7689	.373	1.142	33800	29600	.389	30.8
54	15.94	.0240	.7893	.360	1.149	33625	29300	.389	41.0
55	15.94	.0250	.7923	.375	1.167	34765	29800	.389	41.0
56	20.94	.0253	.7704	.379	1.149	33125	28850	.389	53.8
57	20.97	.0256	.7725	.384	1.157	32250	27900	.389	53.9
58	26.94	.0255	.7719	.382	1.154	30175	26120	.389	66.7
59	26.94	.0250	.7746	.375	1.150	30350	26380	.389	66.7
			3 stiffener panels; 0.040-inch sheet						
60	3.87	0.0383	0.7635	0.575	1.339	38350	28650	0.388	9.97
61	3.86	.0380	.7788	.570	1.349	39425	29230	.388	9.95
62	7.91	.0386	.7590	.579	1.338	36725	27500	.387	20.4
63	7.97	.0390	.7596	.585	1.345	36900	27420	.387	20.6
64	11.91	.0388	.7941	.582	1.376	40000	29100	.388	30.7
65	11.97	.0382	.7800	.573	1.353	38725	28630	.388	30.8
66	15.94	.0398	.7893	.597	1.386	38800	28000	.388	41.1
67	15.94	.0398	.7893	.597	1.386	38680	27900	.388	41.1
68	20.94	.0395	.7941	.592	1.386	38100	27500	.387	54.1
69	20.94	.0395	.7980	.592	1.390	38250	27510	.388	54.0
70	26.91	.0392	.7704	.588	1.358	35550	26200	.385	69.9

TABLE II

Panel Specimens with Bulb Angle 10265

Panel	Panel length (in.)	Sheet thickness (in.)	Bulb angle area (sq.in.)	Sheet area (sq.in.)	Total area (sq.in.)	Ultimate load (lb.)	Average stress σ_a (lb./sq.in.)	ρ	L/ρ
			3 stiffener panels; 0.025-inch sheet						
1	3.75	0.0255	0.283	0.382	0.665	13820	20800	0.302	11.32
2	3.78	.0252	.279	.378	.657	13560	20640	.302	11.42
3	7.94	.0246	.278	.369	.647	12800	19780	.331	24.0
4	7.94	.0245	.278	.368	.646	12760	19730	.331	24.0
5	11.97	.0244	.280	.366	.646	13000	20130	.331	36.2
6	11.97	.0241	.280	.362	.642	12350	19240	.331	36.2
7	15.94	.0250	.280	.375	.655	12500	19090	.331	48.2
8	15.94	.0240	.275	.360	.635	12140	19130	.331	48.2
9	20.94	.0250	.283	.375	.658	12690	19280	.331	63.3
10	20.94	.0246	.281	.369	.650	12100	18620	.331	63.3
11	26.94	.0250	.281	.375	.656	11800	17990	.331	81.5
12	26.94	.0256	.280	.384	.664	12200	18370	.331	81.5
			2 stiffener panels; 0.040-inch sheet						
13	3.91	0.0385	0.189	0.385	0.574	12400	21600	0.325	12.0
14	3.91	.0385	.189	.385	.574	13200	23000	.328	11.92
15	3.94	.0386	.186	.386	.572	12220	21370	.325	12.1
16	7.94	.0389	.191	.389	.580	12030	20740	.323	24.7
17	7.98	.0387	.191	.387	.578	12275	21250	.324	24.6
18	11.97	.0390	.193	.390	.583	12225	21000	.322	37.1
19	12.0	.0390	.193	.390	.583	12625	21670	.326	39.1
20	15.97	.0380	.194	.380	.574	12800	22310	.327	48.8
21	15.94	.0375	.194	.375	.569	12520	22020	.327	48.7
22	20.95	.0391	.186	.391	.577	11150	19310	.319	65.6
23	20.94	.0385	.185	.385	.570	10735	18820	.318	65.8
24	26.97	.0390	.187	.390	.577	1750	18620	.318	84.7
25	26.94	.0390	.186	.390	.6				
			3 stiffener panels; 0.040-inch sheet						
26	3.72	0.0382	0.280	0.573	0.853	18995	22300	0.327	11.4
27	7.97	.0397	.282	.595	.877	17625	20100	.326	24.4
28	7.94	.0391	.279	.586	.867	17350	20000	.327	24.3
29	11.97	.0390	.282	.585	.867	16925	19520	.325	36.8
30	11.97	.0384	.281	.576	.857	17000	19830	.326	36.7
31	15.97	.0395	.274	.592	.866	17020	19670	.330	48.4
32	15.94	.0389	.276	.584	.860	16700	19420	.323	49.4
33	20.87	.0392	.279	.588	.867	15390	17750	.318	65.6
34	20.87	.0388	.284	.582	.866	17100	19760	.325	64.2
35	26.94	.0382	.280	.573	.853	15740	18460	.320	84.1
36	26.94	.0383	.275	.575	.850	16000	18830	.321	83.9
			4 stiffener panels; 0.040-inch sheet						
37	3.94	0.0370	0.377	0.740	1.117	24075	21590	0.32	12.32
38	7.87	.0372	.383	.744	1.127	23425	20820	.326	24.13
39	7.95	.0378	.376	.756	1.132	22820	20130	.3247	24.50
40	11.97	.0380	.386	.760	1.146	22900	20530	.322	37.15
41	11.90	.0381	.387	.762	1.149	23700	20640	.326	36.50
42	15.94	.0388	.374	.776	1.150	21875	19020	.3265	50.40
43	15.94	.0382	.368	.764	1.132	22000	19420	.3265	50.40
44	20.87	.0373	.3692	.746	1.115	20930	18780	.3234	66.50
45	20.91	.0371	.3716	.742	1.114	20825	18700	.3226	64.80
46	26.94	.0371	.3728	.742	1.115	20525	18400	.3210	83.90
47	26.94	.0378	.3724	.756	1.128	20000	17760	.3190	84.40

TABLE IV

Panel Specimens with Bulb Angle 8478

Panel	Panel length (in.)	Sheet thickness (in.)	Bulb angle area (sq.in.)	Sheet area (sq.in.)	Total area (sq.in.)	Ultimate load (lb.)	Average stress σ_a (lb./sq.in.)	ρ	L/ρ
			3 stiffener panels; 0.025-inch sheet						
71	3.85	0.0253	0.4707	0.379	0.850	20680	24320	0.411	9.37
72	3.82	.0253	.4710	.379	.850	20590	24220	.411	9.30
73	7.94	.0252	.4698	.378	.848	19710	23240	.412	19.3
74	7.94	.0250	.4698	.375	.845	19300	22850	.412	19.3
75	11.94	.0245	.4680	.367	.835	18480	22130	.411	29.1
76	11.94	.0252	.5016	.378	.880	19010	21600	.411	29.1
77	15.91	.0259	.5163	.388	.904	19800	21900	.411	38.8
78	15.91	.0245	.5163	.367	.883	19600	22200	.411	38.8
79	20.94	.0254	.5166	.381	.898	18700	20810	.410	51.0
80	20.97	.0256	.516	.384	.900	17200	19110	.408	51.3
81	26.87	.0252	.5097	.378	.888	18700	21060	.410	65.5
82	26.91	.0249	.5109	.373	.884	18400	20810	.410	65.6
			3 stiffener panels; 0.040-inch sheet						
83	3.75	0.0385	0.486	0.577	1.063	24500	23020	-	-
84	3.95	.0380	.484	.570	1.054	22090	20930	0.403	9.80
85	7.94	.0391	.491	.586	1.077	23800	22120	.408	19.4
86	7.94	.0390	.484	.585	1.069	23900	22390	.409	19.4
87	11.85	.0380	.487	.570	1.057	22590	21390	.405	29.3
88	11.94	.0388	.480	.582	1.062	22420	21110	.404	29.6
89	15.94	.0375	.482	.562	1.044	20950	20080	.400	39.8
90	15.87	.0395	.503	.592	1.095	23100	21100	.404	39.2
91	20.91	.0390	.519	.585	1.104	23175	21000	.403	51.8
92	20.87	.0392	.519	.588	1.107	20675	18690	.395	52.9
93	26.84	.0382	.503	.573	1.076	21240	19750	.399	67.5
94	26.87	.0393	.476	.590	1.066	21540	20200	.401	67.0

TABLE VI

Panel Specimens with Bulb Angle 10266

Panel	Panel length (in.)	Sheet thickness (in.)	Bulb angle area (sq.in.)	Sheet area (sq.in.)	Total area (sq.in.)	Ultimate load (lb.)	Average stress σ_a (lb./sq.in.)	ρ	L/ρ
			2 stiffener panels; 0.020-inch sheet						
130	2.94	0.020	0.2418	0.20	0.442	10570	23920	0.365	8.06
131	5.38	.020	.2418	.20	.442	10325	23400	.365	14.76
132	11.0	.020	.2418	.20	.442	10000	22660	.365	30.2
133	16.32	.020	.2418	.20	.442	10400	23550	.365	44.8
134	22.38	.020	.2418	.20	.442	9985	22600	.365	61.4
135	27.5	.020	.2418	.20	.442	8535	19300	.365	75.4
			3 stiffener panels; 0.020-inch sheet						
136	2.88	0.020	0.3627	0.300	0.663	15120	22840	0.365	7.90
137	5.28	.020	.3627	.300	.663	15700	23700	.365	14.48
138	11.0	.020	.3627	.300	.663	14900	22500	.365	30.2
139	16.38	.020	.3627	.300	.663	15720	23740	.365	44.9
140	22.38	.020	.3627	.300	.663	13710	20700	.365	61.4
141	27.63	.020	.3627	.300	.663	12200	18410	.365	75.8
			4 stiffener panels; 0.020-inch sheet						
142	2.88	0.020	0.4836	0.400	0.884	21300	24100	0.365	7.90
143	5.35	.020	.4836	.400	.884	20025	22650	.365	14.67
144	11.34	.020	.4836	.400	.884	18900	21400	.365	31.1
145	16.44	.020	.4836	.400	.884	19800	22400	.365	45.1
146	22.38	.020	.4836	.400	.884	18750	21220	.365	61.4
147	27.63	.020	.4836	.400	.884	16400	18570	.365	75.8

TABLE V

Panel Specimens with Bulb Angle 8476

Panel	Panel length (in.)	Sheet thickness (in.)	Bulb angle area (sq.in.)	Sheet area (sq.in.)	Total area (sq.in.)	Ultimate load (lb.)	Average stress σ_a (lb./sq.in.)	ρ	L/ρ
			2 stiffener panels; 0.040-inch sheet						
95	4	0.039	0.296	0.390	0.686	14150	20630	0.563	7.1
96	4	.042	.292	.420	.712	15875	22310	.563	7.1
97	8	.039	.298	.390	.688	12800	18780	.563	14.2
98	8	.042	.300	.420	.720	13900	19310	.563	21.3
99	12	.039	.304	.390	.694	13175	18980	.563	21.3
100	16	.040	.304	.400	.704	12600	17900	.563	28.4
101	16	.040	.296	.400	.696	12700	18240	.563	28.4
102	20.87	.041	.300	.410	.710	12380	17280	.562	37.2
103	20.87	.041	.300	.410	.710	12275	17280	.562	37.2
104	27	.040	.298	.400	.698	12075	17300	.565	47.8
105	27	.043	.292	.430	.722	12405	17200	.565	47.8
			3 stiffener panels; 0.040-inch sheet						
106	4	0.041	0.450	0.615	1.065	22100	20730	0.563	7.1
107	4	.041	.444	.615	1.059	22850	21600	.563	7.1
108	8	.042	.444	.630	1.074	20670	19260	.563	14.2
109	8	.042	.444	.630	1.074	20225	18870	.563	14.2
110	12	.040	.444	.600	1.044	18950	18100	.563	21.3
111	12	.041	.456	.615	1.071	19875	18530	.563	21.3
112	16	.039	.450	.585	1.035	18050	17430	.563	28.4
113	16	.039	.450	.585	1.035	17820	17230	.563	28.4
114	21	.040	.444	.600	1.044	17100	16380	.565	37.2
115	21	.040	.444	.600	1.044	17100	16380	.565	37.2
116	26.87	.040	.450	.600	1.050	17100	16210	.562	47.8
117	27.00	.038	.453	.570	1.023	16800	16410	.565	47.8
			4 stiffener panels; 0.040-inch sheet						
118	4	0.042	0.592	0.840	1.432	29000	20250	0.563	7.1
119	4	.042	.600	.840	1.440	29450	20450	.563	7.1
120	8	.041	.592	.820	1.412	25670	18180	.563	14.2
121	8	.040	.592	.800	1.392	24725	17740	.563	14.2
122	12	.042	.600	.840	1.440	25000	17370	.563	21.3
123	12	.041	.612	.820	1.432	23975	16780	.563	21.3
124	16	.042	.600	.840	1.440	25000	17370	.563	28.4
125	16	.042	.596	.840	1.436	24450	17030	.563	28.4
126	21	.041	.596	.820	1.416	23800	16810	.565	37.2
127	21	.039	.592	.780	1.372	23080	16800	.565	37.2
128	27	.040	.600	.800	1.400	22000	15720	.565	47.8
129	27	.041	.600	.820	1.420	23100	16250	.565	47.8

TABLE VII

Panel Specimens with Bulb Angle 10282

Panel	Panel length (in.)	Sheet thickness (in.)	Bulb angle area (sq.in.)	Sheet area (sq.in.)	Total area (sq.in.)	Ultimate load (lb.)	Average stress σ_a (lb./sq.in.)	ρ	L/ρ
			2 stiffener panels; 0.020-inch sheet						
148	3.0	0.02	0.1294	0.16	0.289	6250	21600	0.278	10.9
149	5.5	.02	.1294	.16	.289	6550	22640	.278	19.8
150	11.0	.02	.1294	.16	.289	5310	18350	.278	39.6
151	16.5	.02	.1294	.16	.289	6170	21300	.278	59.4
152	22.0	.02	.1294	.16	.289	6160	21300	.278	79.2
153	27.5	.02	.1294	.16	.289	5040	17400	.278	98.2
			2 stiffener panels; 0.040-inch sheet						
154	3.0	0.04	0.1294	0.32	0.449	9460	21050	0.332	9.04
155	5.5	.04	.1294	.32	.449	11080	24700	.332	16.6
156	11.0	.04	.1294	.32	.449	9150	20360	.332	33.2
157	16.5	.04	.1294	.32	.449	10080	22470	.332	49.7
158	22.0	.04	.1294	.32	.449	11150	24800	.332	66.3
159	27.5	.04	.1294	.32	.449	9830	21900	.332	82.4
			3 stiffener panels; 0.020-inch sheet						
160	3.0	0.02	0.1941	0.24	0.434	7860	18100	0.278	10.9
161	5.5	.02	.1941	.24	.434	9390	21630	.278	19.8
162	11.0	.02	.1941	.24	.434	7675	17680	.278	39.6
163	16.5	.02	.1941	.24	.434	8915	20530	.278	59.4
164	22.	.02	.1941	.24	.434	7602	17500	.278	79.2
165	27.5	.02	.1941	.24	.434	6650	15320	.278	98.2
			3 stiffener panels; 0.040-inch sheet						
166	3.0	0.04	0.1941	0.48	0.674	16170	23970	0.332	9.04
167	5.5	.04	.1941	.48	.674	12290	18230	.332	16.6
168	11.0	.04	.1941	.48	.674	12870	19090	.332	33.2
169	16.5	.04	.1941	.48	.674	14012	20780	.332	49.7
170	22.0	.04	.1941	.48	.674	14938	22160	.332	66.3
171	27.5	.04	.1941	.48	.674	12240	18150	.332	82.4
			4 stiffener panels; 0.020-inch sheet						
172	3.0	0.02	0.2588	0.32	0.5788	11855	20500	0.278	10.9
173	5.5	.02	.2588	.32	.5788	11450	19780	.278	19.8
174	11.0	.02	.2588	.32	.5788	8720	15060	.278	39.6
175	16.5	.02	.2588	.32	.5788	11390	19670	.278	59.4
176	22.0	.02	.2588	.32	.5788	9985	17260	.278	79.2
177	27.5	.02	.2588	.32	.5788	8810	15220	.278	98.2
			4 stiffener panels; 0.040-inch sheet						
178	3.0	0.04	0.2588	0.64	0.8988	18200	20250	0.332	9.04
179	5.5	.04	.2588	.64	.8988	20230	22500	.332	16.6
180	11.0	.04	.2588	.64	.8988	17120	19050	.332	33.2
181	16.5	.04	.2588	.64	.8988	18590	20670	.332	49.7
182	22.0	.04	.2588	.64	.8988	17938	19960	.332	66.3
183	27.5	.04	.2588	.64	.8988	14825	16500	.332	82.4

TABLE VIII

Pin-End Tests - Stiffeners without Sheet

Bulb-angle specimen	Area (sq.in.)	ρ	Length L (in.)	L/ρ	Ultimate load (lb.)	Ultimate stress (lb./sq.in.)
10265	0.0931	0.110	24.24	220	196	2105
			18.73	170	335	3595
			13.21	120	615	6610
			7.62	69.3	1540	16550
10282	0.0647	0.116	24.24	209	147	2275
			18.73	161.5	210	3250
			13.21	114	410	6340
			7.62	65.7	1025	15870
3046	0.1252	0.1143	24.24	212	294	2345
			18.73	164	405	3240
			13.21	115.5	700	5600
			7.62	66.6	1945	15520
5436	0.2470	0.218	24.24	111.2	2230	9030
			18.73	85.9	3495	14140
			13.21	60.6	6040	24450
			7.62	35.0	9605	38900
12224	0.1709	0.143	24.24	169.5	820	4800
			18.73	131.0	1180	6900
			13.21	92.4	2320	13590
			7.62	53.3	5840	34200
8477	0.2774	0.242	24.24	100.2	2703	9775
			18.73	75.7	4310	15520
			13.21	54.7	7365	26550
			7.62	31.5	10370	37400
8476	0.1501	0.149	24.24	162.4	590	3930
			18.73	125.7	875	5830
			13.21	88.7	1570	11120
			7.62	51.1	4020	26800
8478	0.1679	0.228	24.24	106.2	1490	8870
			18.73	82.1	2275	13540
			13.21	57.9	3875	22450
			7.62	33.4	5770	34400

TABLE VIII (Continued)

Pin-End Tests - Stiffeners without Sheet

Bulb-angle specimen	Area (sq.in.)	ρ	Length L (in.)	L/ρ	Ultimate load (lb.)	Ultimate stress (lb./sq.in.)
10266	0.1220	0.155	24.24	156.3	469	3845
			18.73	120.8	775	6350
			13.21	85.2	1545	12670
			7.62	49.1	2650	21700
4200	0.1334	0.156	24.24	155.0	621	4650
			18.73	120.0	955	7160
			13.21	84.8	1900	14250
			7.62	48.9	4280	32050
766	0.0856	0.1165	24.24	208.0	260	3040
			18.73	161.0	385	4500
			13.21	113.3	705	8240
			7.62	65.4	2005	23450
12678	0.04023	0.104	24.24	233.0	107	2675
			18.73	180.0	155	3880
			13.21	127.0	305	7615
			7.62	73.3	710	17750

TABLE IX

Specimens of Bent-up Angle Stiffeners

(L.S. 106-0.051; 6 stiffener panels; 15 inches wide; 0.064-inch sheet; 5-inch stiffener spacing)

Panel	Panel length	Sheet thickness (in.)	Stiffener area (sq.in.)	Sheet area (sq.in.)	Total area (sq.in.)	Ultimate load (lb.)	Average stress (lb./sq. in.)
A	16	0.0632	0.407	0.947	1.354	28950	21400
B	16	.0630	.404	.945	1.349	28600	21210
C	16	.0626	.406	.939	1.345	28450	21150

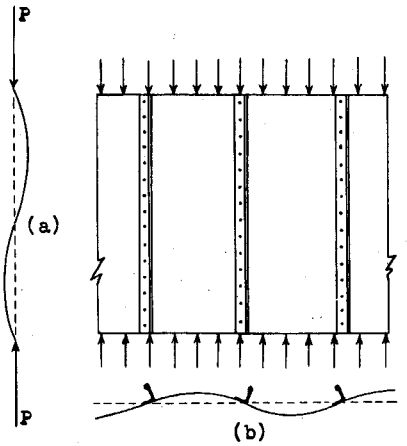

Figure 1.- The panel with sheet buckled.

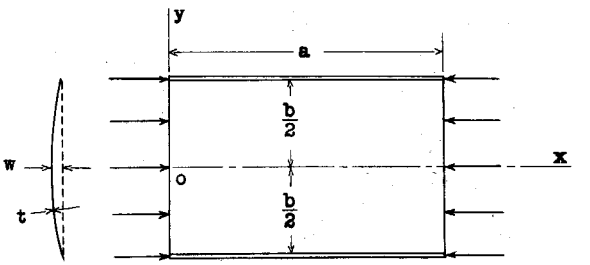

Figure 2.- A rectangular plate with elastic supports.

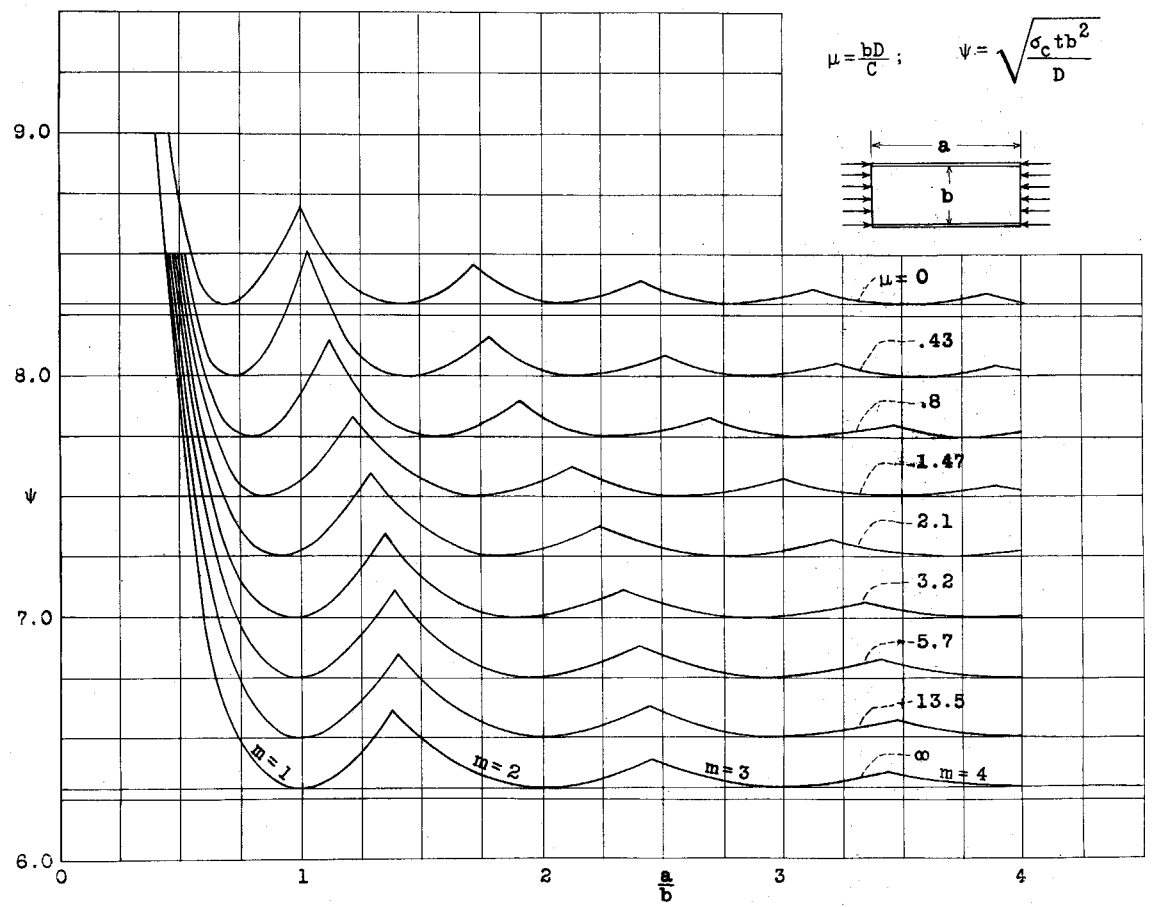

Figure 3.- Graphical solution of equation (14).

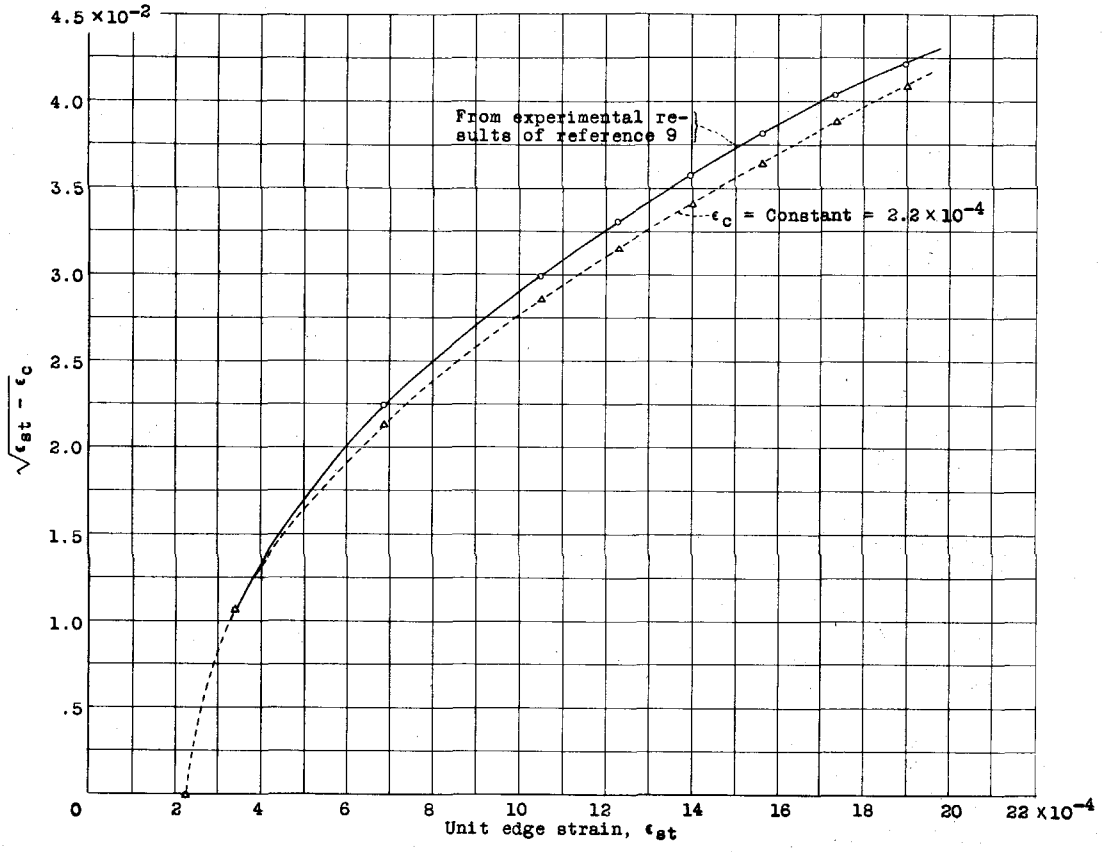

Figure 4.- Variation of ϵ_{st} with $\sqrt{\epsilon_{st}-\epsilon_c}$

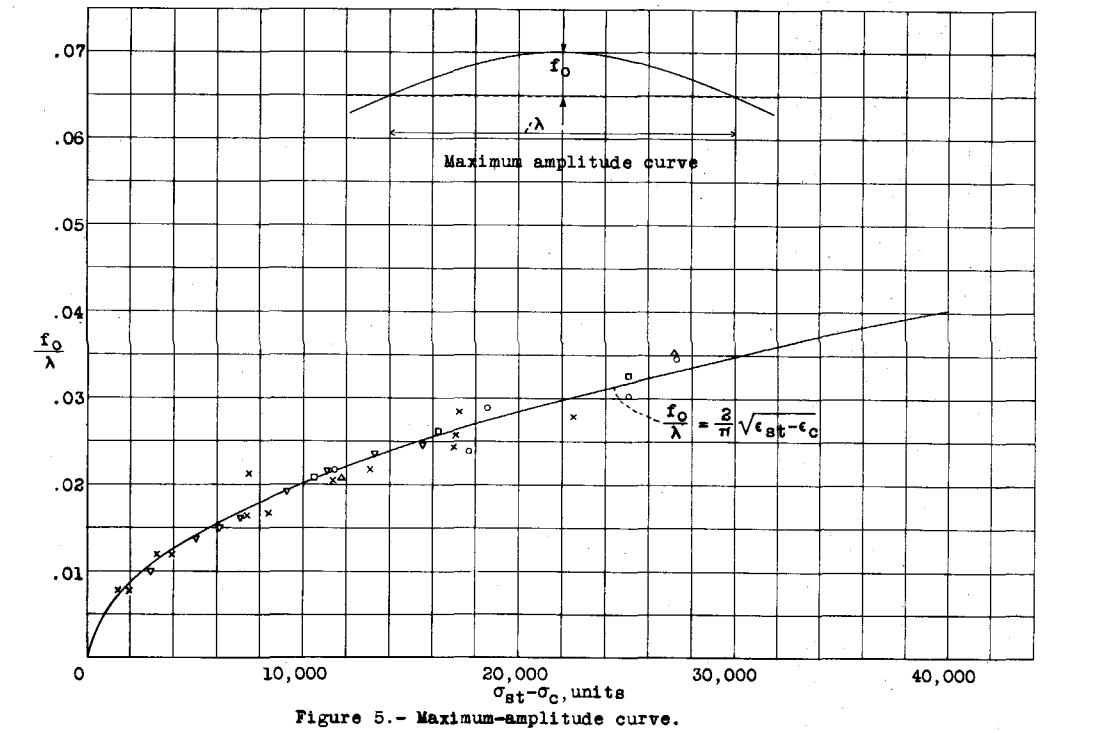

Figure 5.- Maximum-amplitude curve.

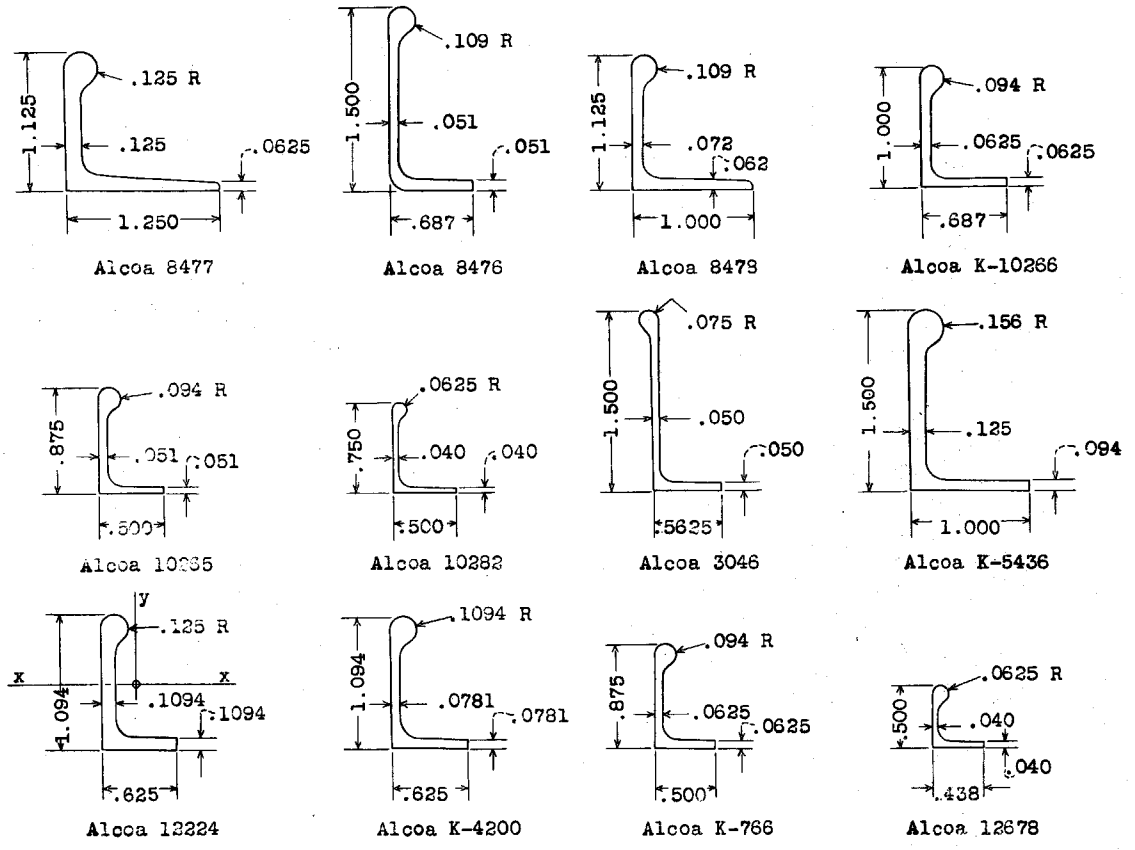

Figure 6.- Bulb-angle test specimens. All dimensions in inches.

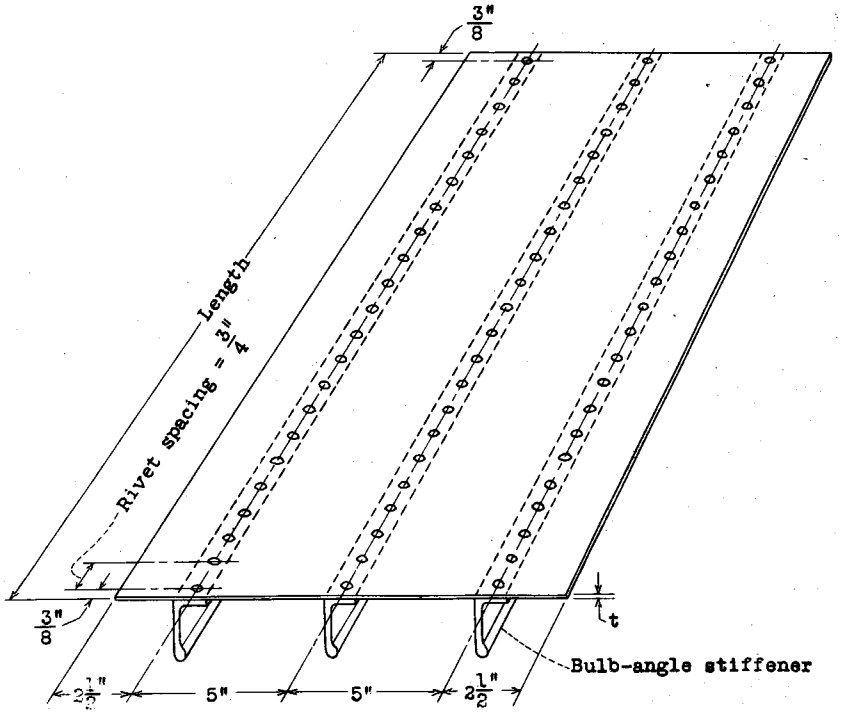

Figure 8.- Construction of typical panel specimen.

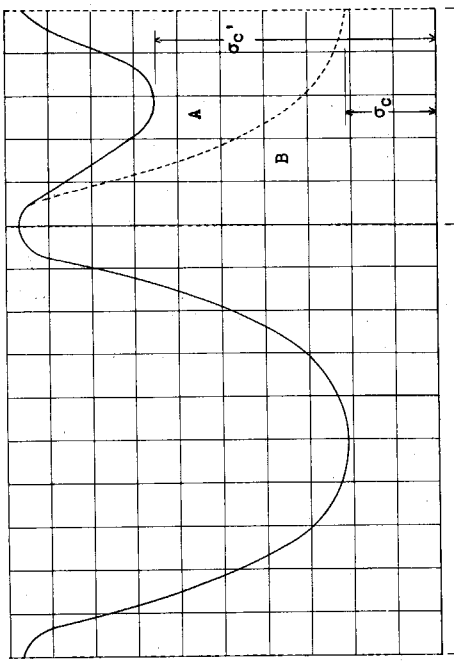

Figure 13.- Typical stress distribution showing the effect of the tube edge support, $k_1 = A/B$.

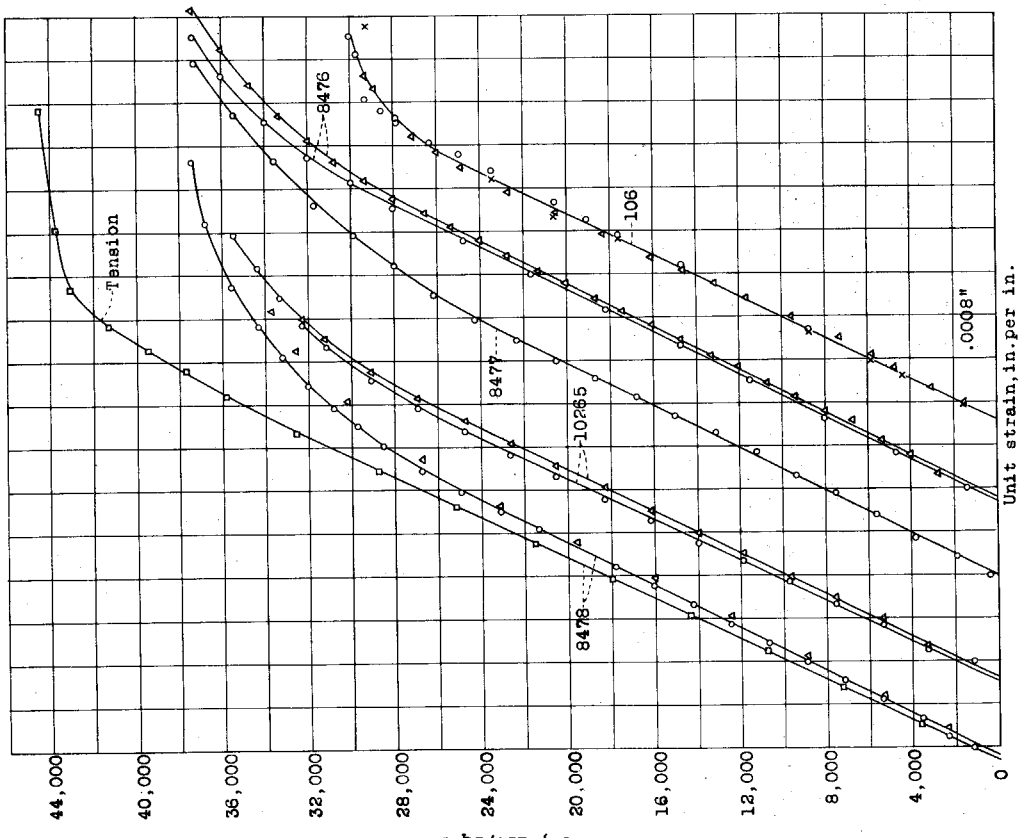

Figure 7.- Strength properties of stiffeners.

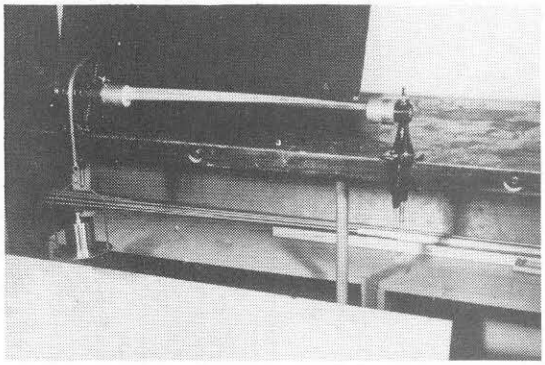

Figure 12.- Torsion-test set-up.

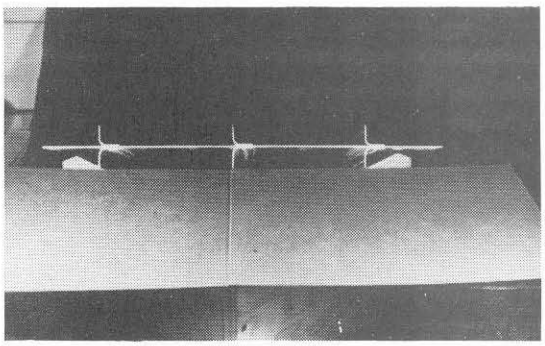

Figure 41.- Specimen A.

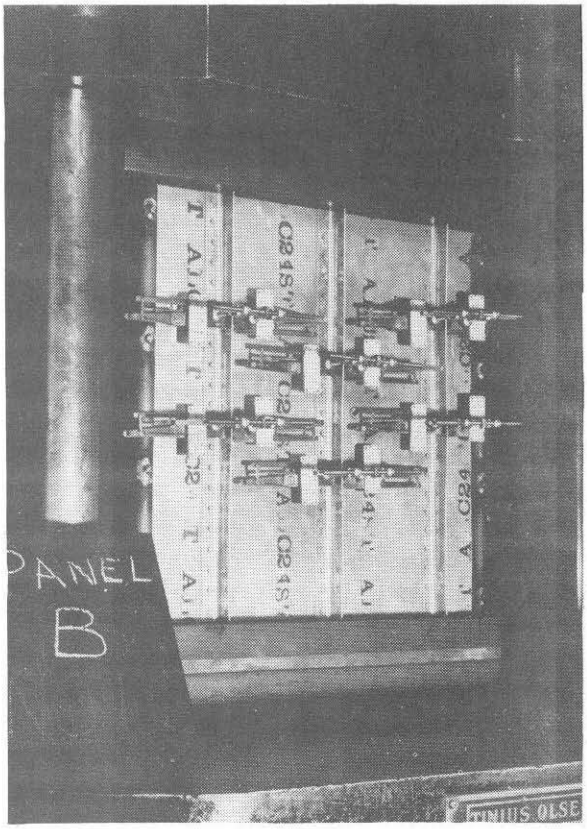

Figure 10.- Test specimen showing mounted instruments.

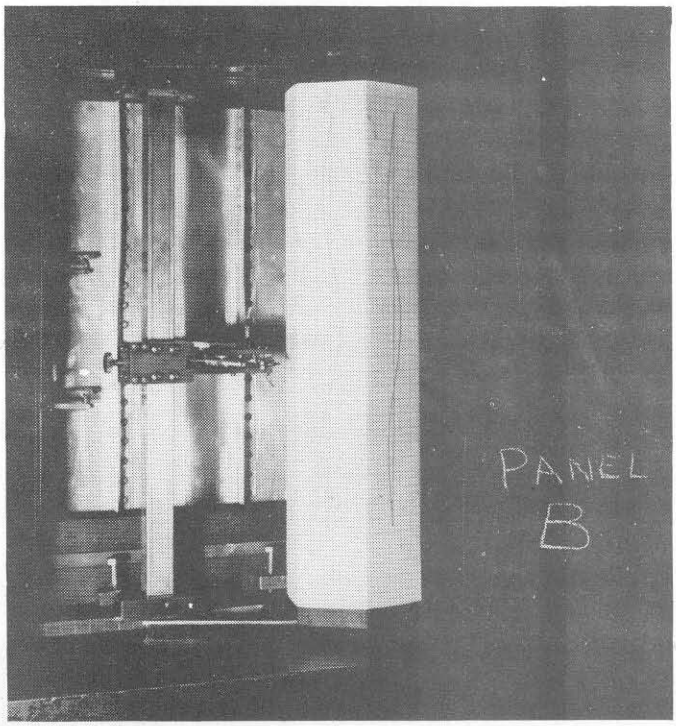

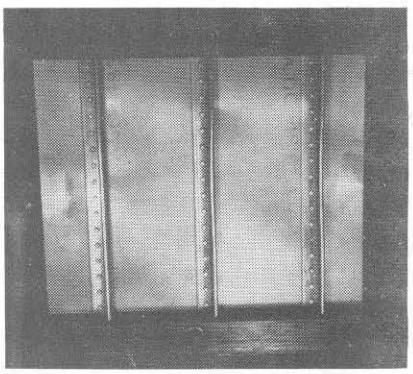

Figure 9.- Panel test specimen.

Figure 11.- Contour-tracing machine.

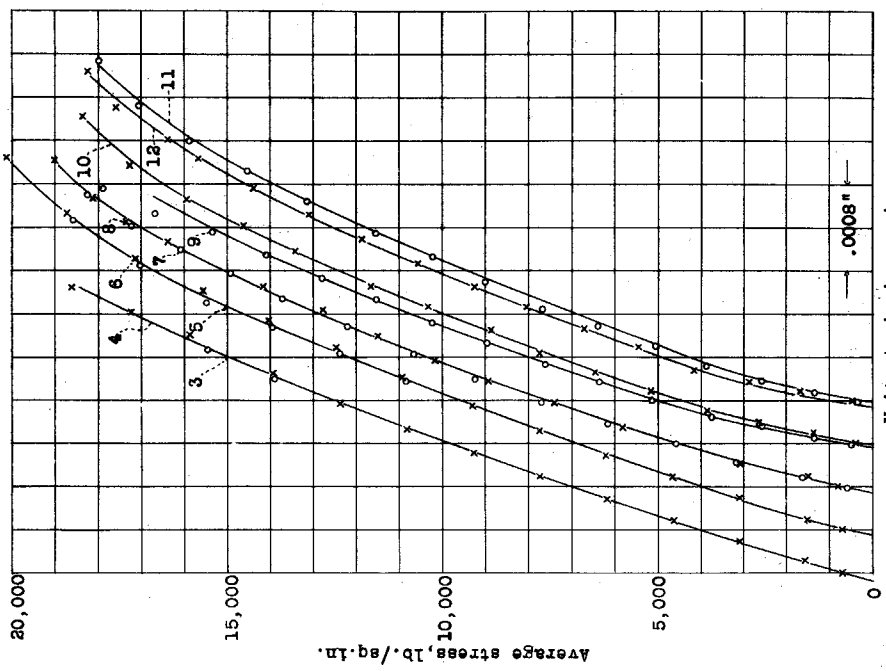

Figure 15.- Stress-strain curves for three stiffener panels. 0.025"-24ST alclad skin; bulb angle 10265.

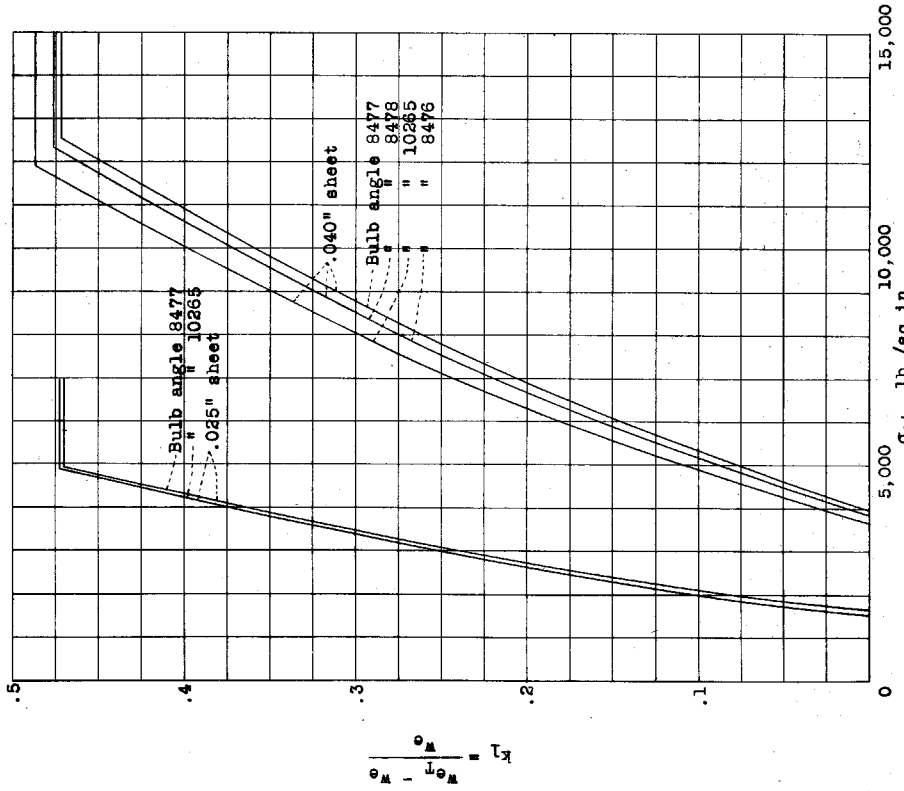

Figure 14.- Variation of k_1, with stiffener stress.

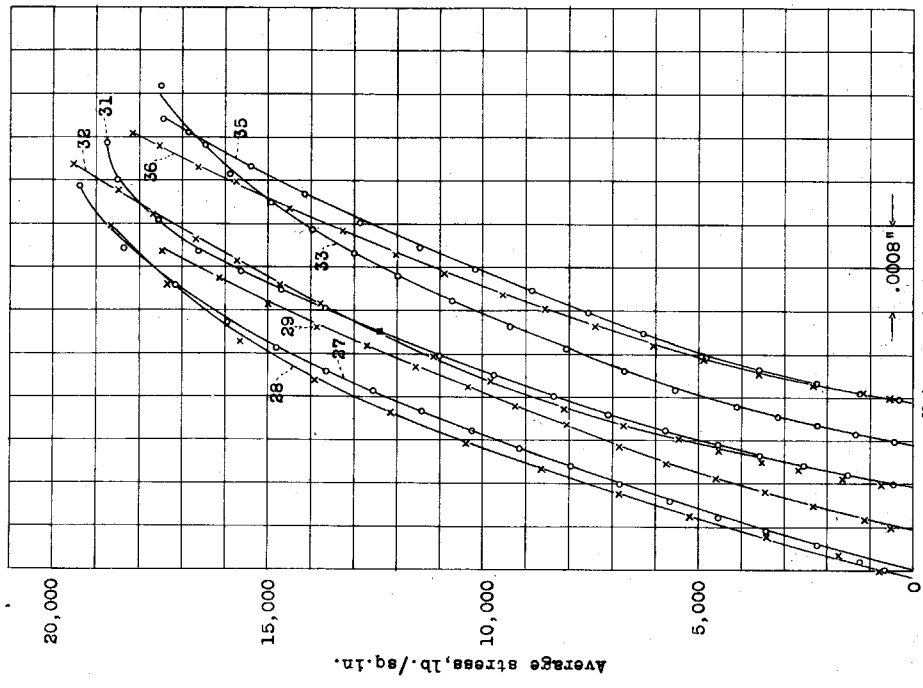

Figure 16.- Stress-strain curves for two stiffener panels. 0.040"-24ST alclad skin; bulb angle 10265.

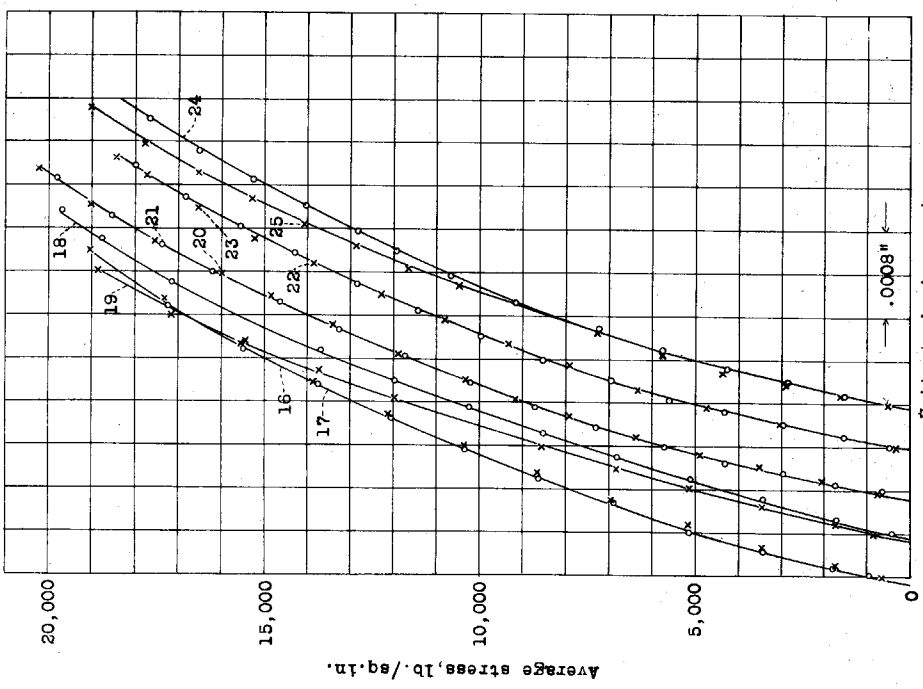

Figure 17.- Stress-strain curves for three stiffener panels. 0.040"-24ST alclad skin; bulb angle 10265.

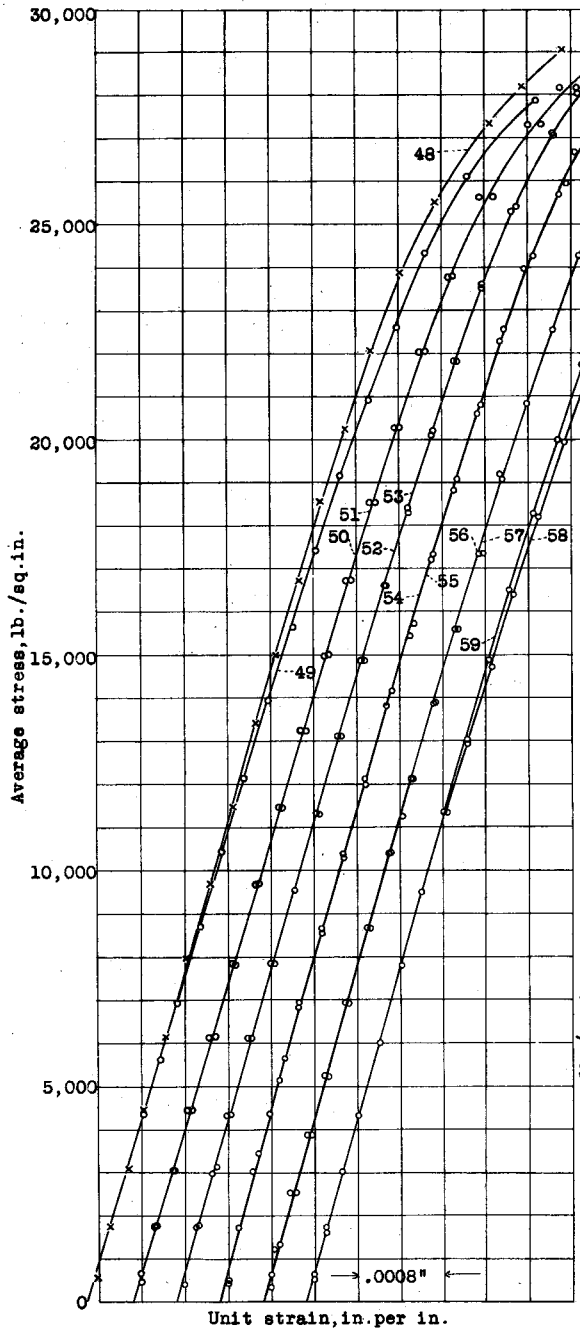

Figure 19.- Stress-strain curves for three stiffener panels. 0.025"-24ST alclad skin; bulb angle 8477.

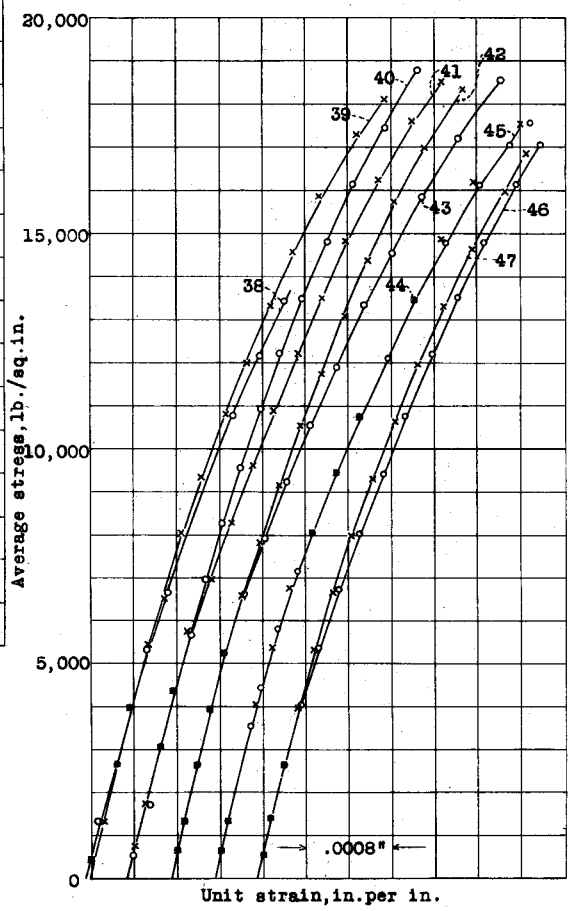

Figure 18.- Stress-strain curves for four stiffener panels. 0.040"-24ST alclad skin; bulb angle 10265.

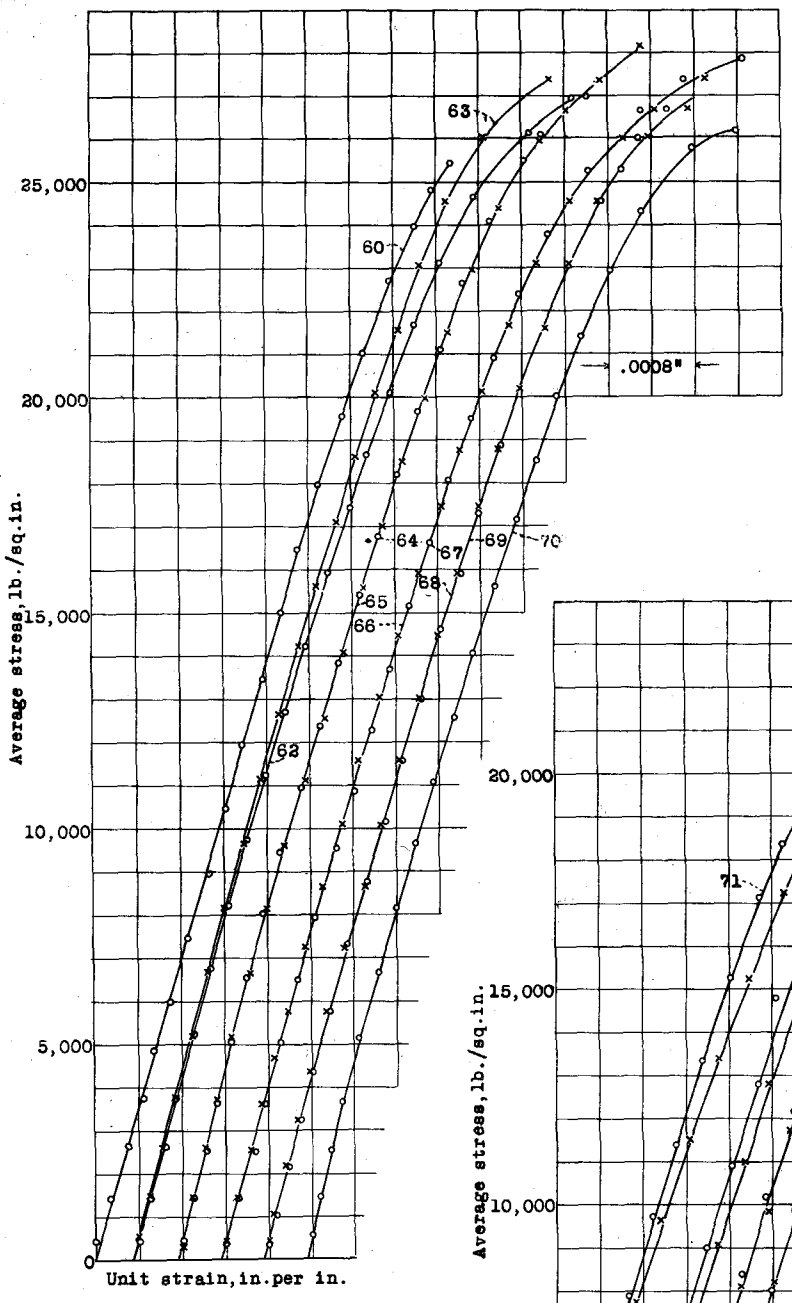

Figure 20.- Strain-strain curves for three stiffener panels. 0.040"-24ST alclad skin; bulb angle 8477.

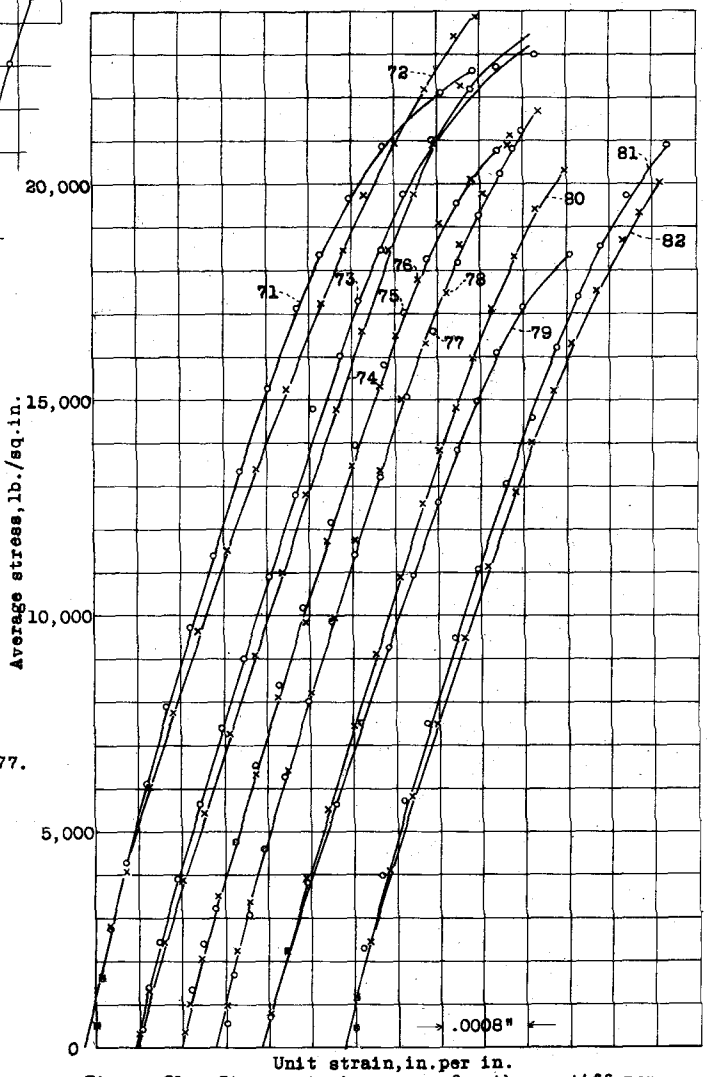

Figure 21.- Stress-strain curves for three stiffener panels. 0.025"-24ST alclad skin; bulb angle 8478.

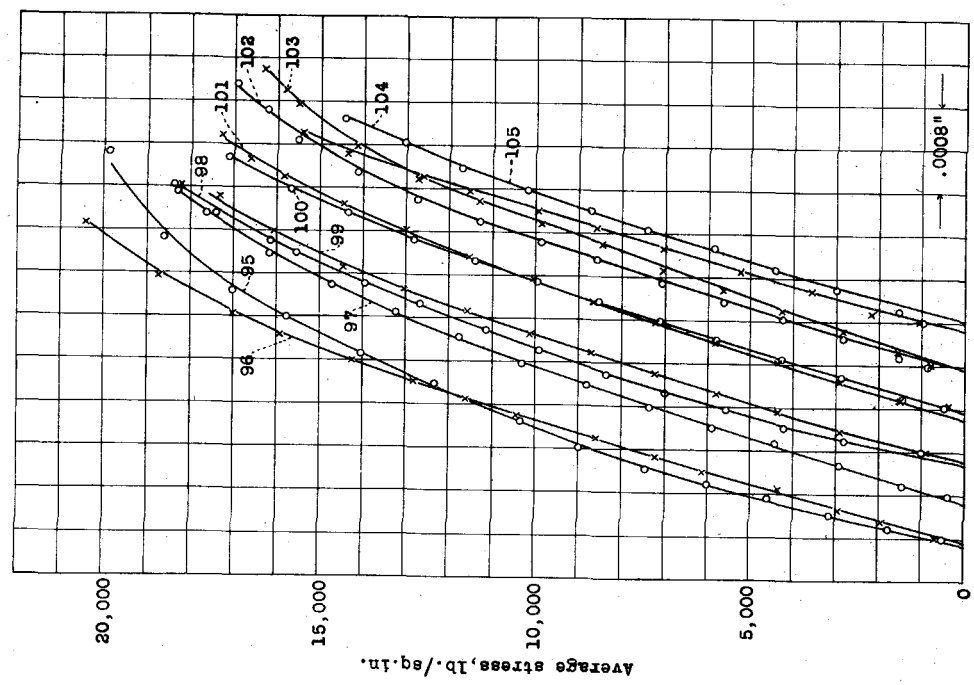

Figure 23.- Stress-strain curves for two stiffener panels. 0.040"-24ST alclad skin; bulb angle 8476.

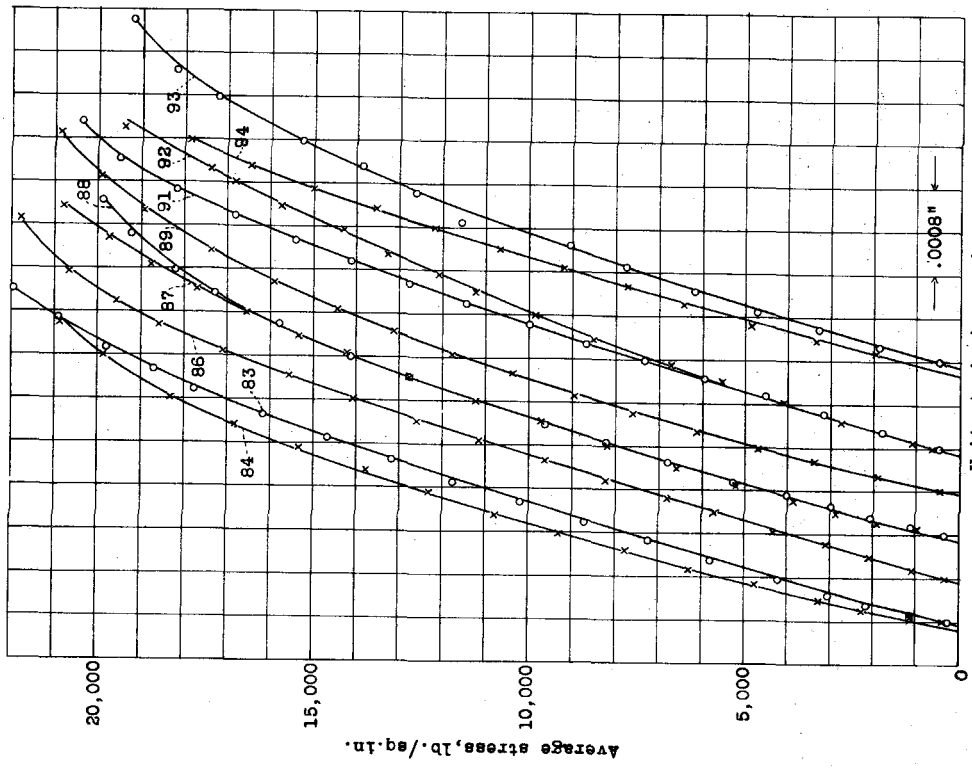

Figure 22.- Stress-strain curves for three stiffener panels. 0.040"-24ST alclad skin; bulb angle 8478.

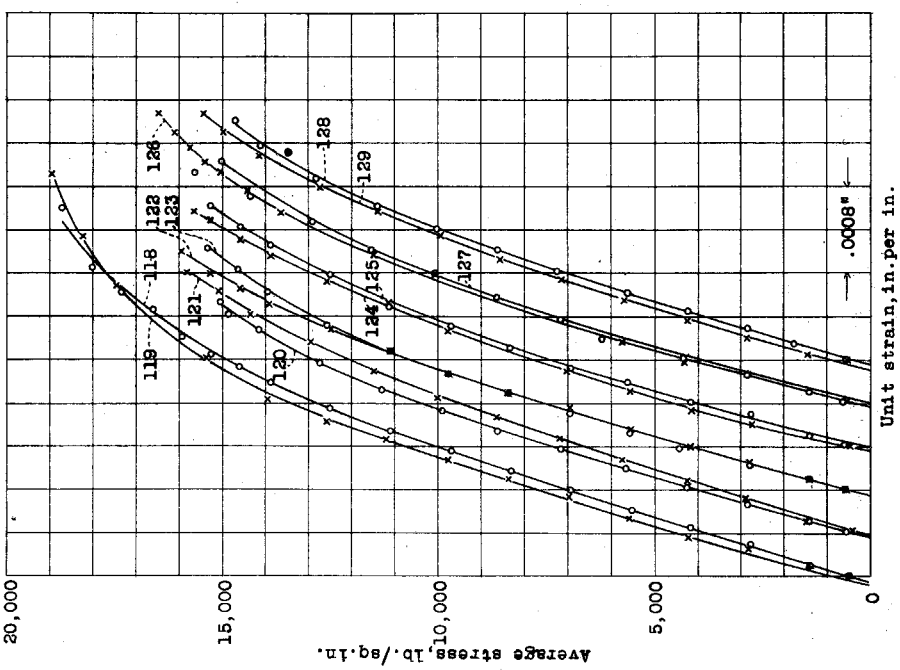

Figure 25.- Stress-strain curves for four stiffener panels. 0.040"-24ST alclad skin; bulb angle 8476.

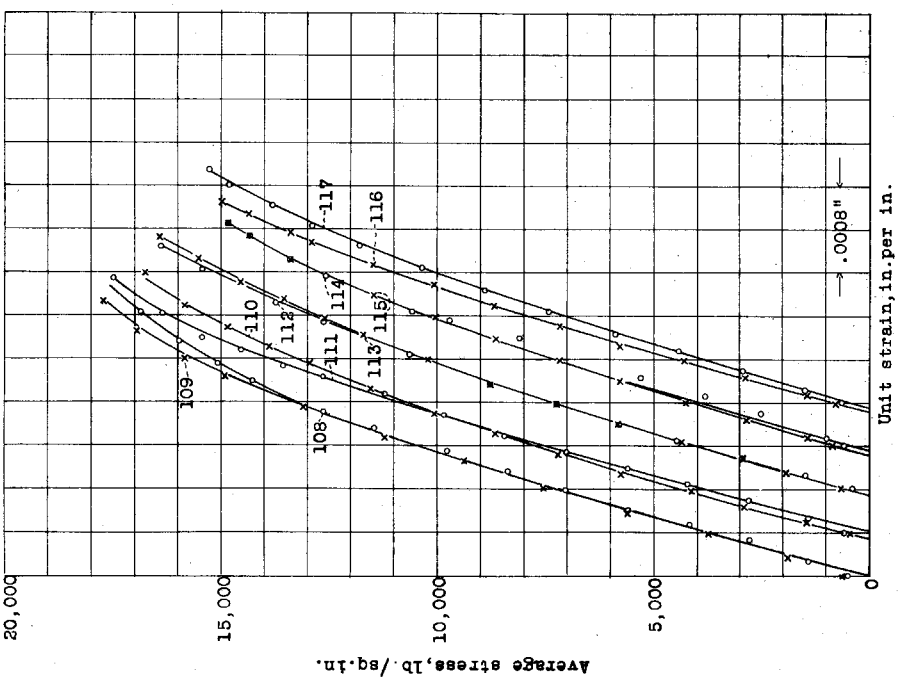

Figure 24.- Stress-strain curves for three stiffener panels: 0.040"-24ST alclad skin; bulb angle 8476.

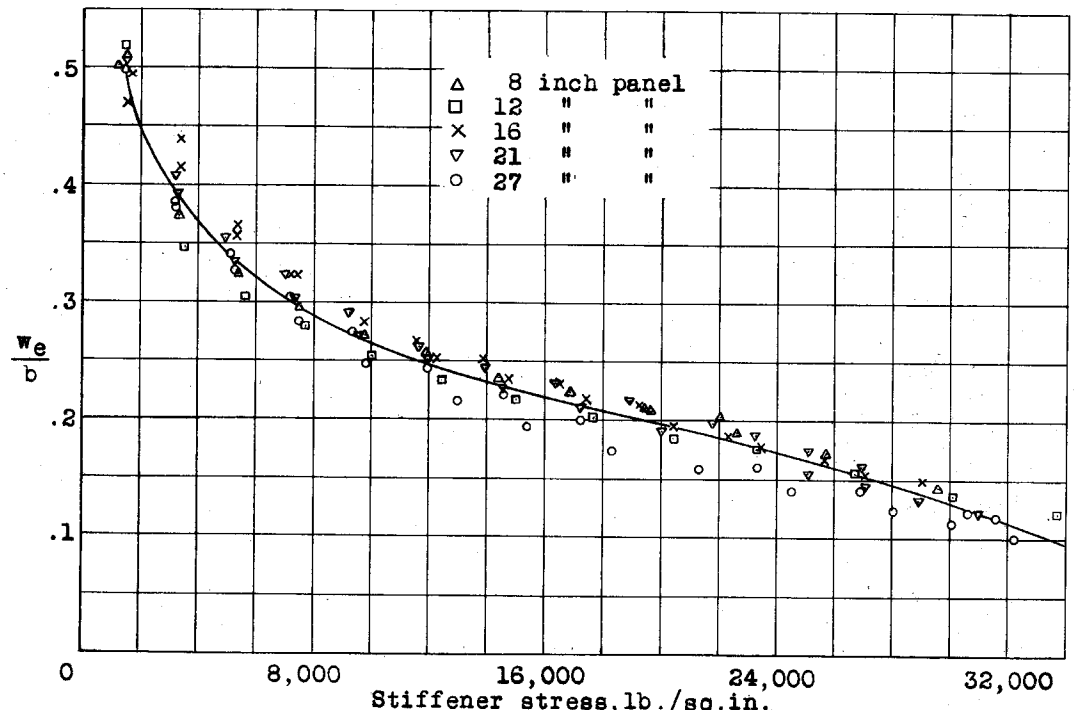

Figure 26.- Effective-width curve for three stiffener panels. 0.025"-24ST alclad skin; bulb angle 10265.

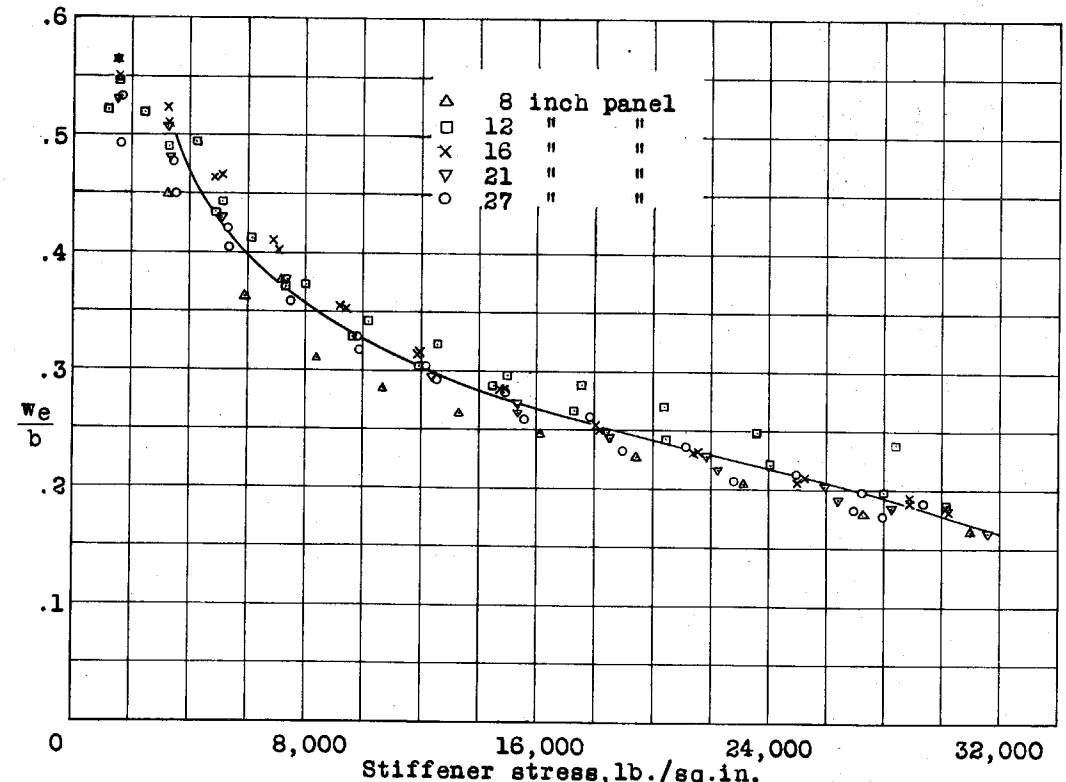

Figure 27.- Effective-width curve for two stiffener panels. 0.040"-24ST alclad skin; bulb angle 10265.

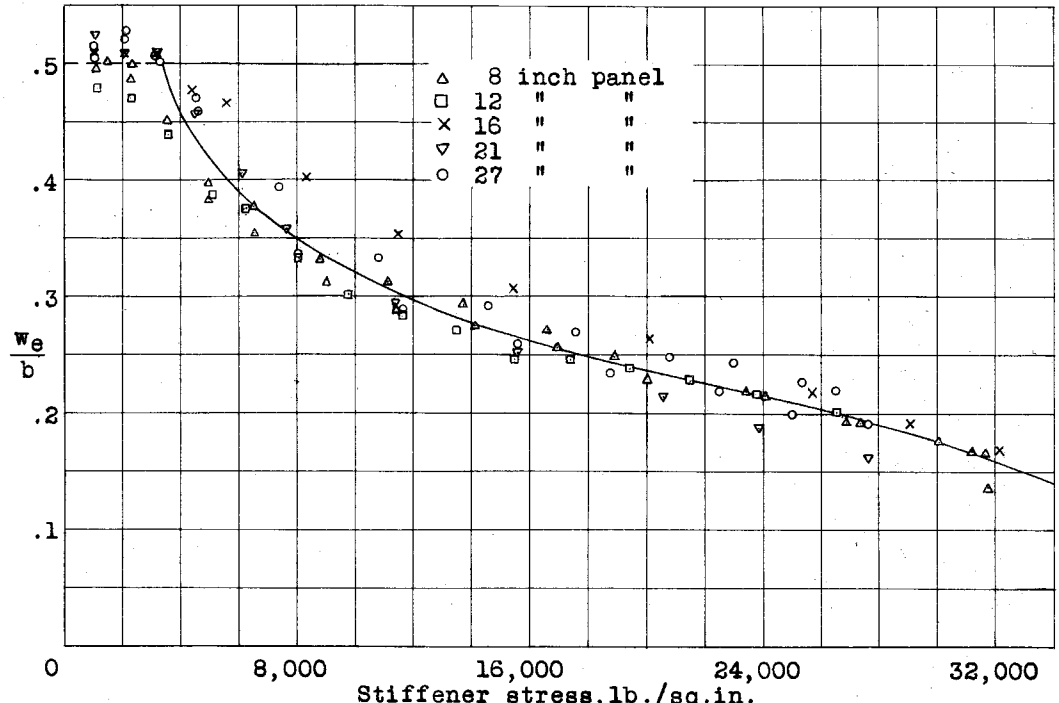

Figure 28.- Effective-width curve of three stiffener panels. 0.040"-24ST alclad skin; bulb angle 10265.

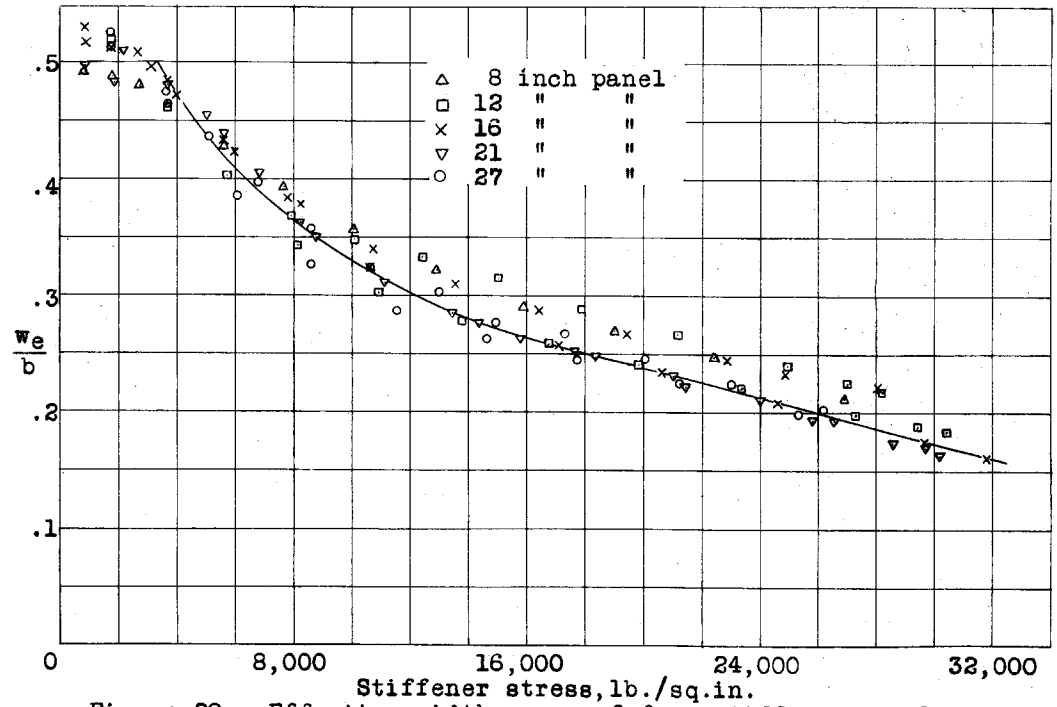

Figure 29.- Effective-width curve of four stiffener panels. 0.040"-24ST alclad skin; bulb angle 10265.

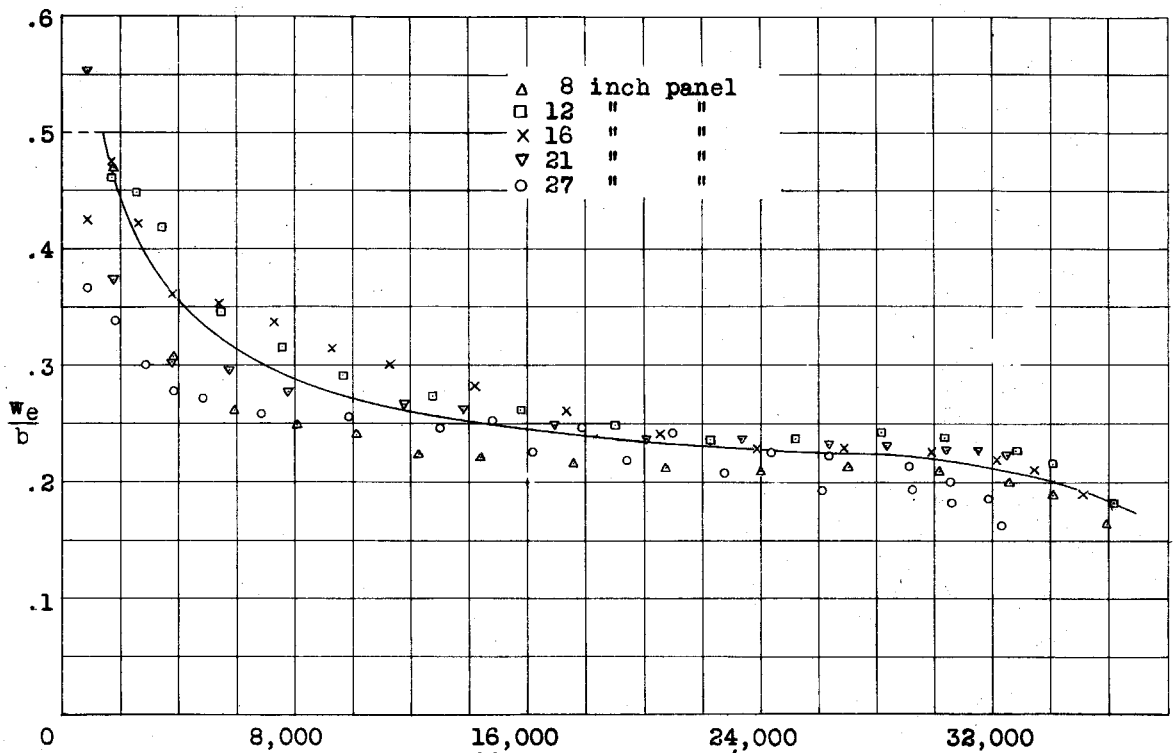

Figure 30.- Effective-width curve of three stiffener panels. 0.025"-24ST alclad skin; bulb angle 8477.

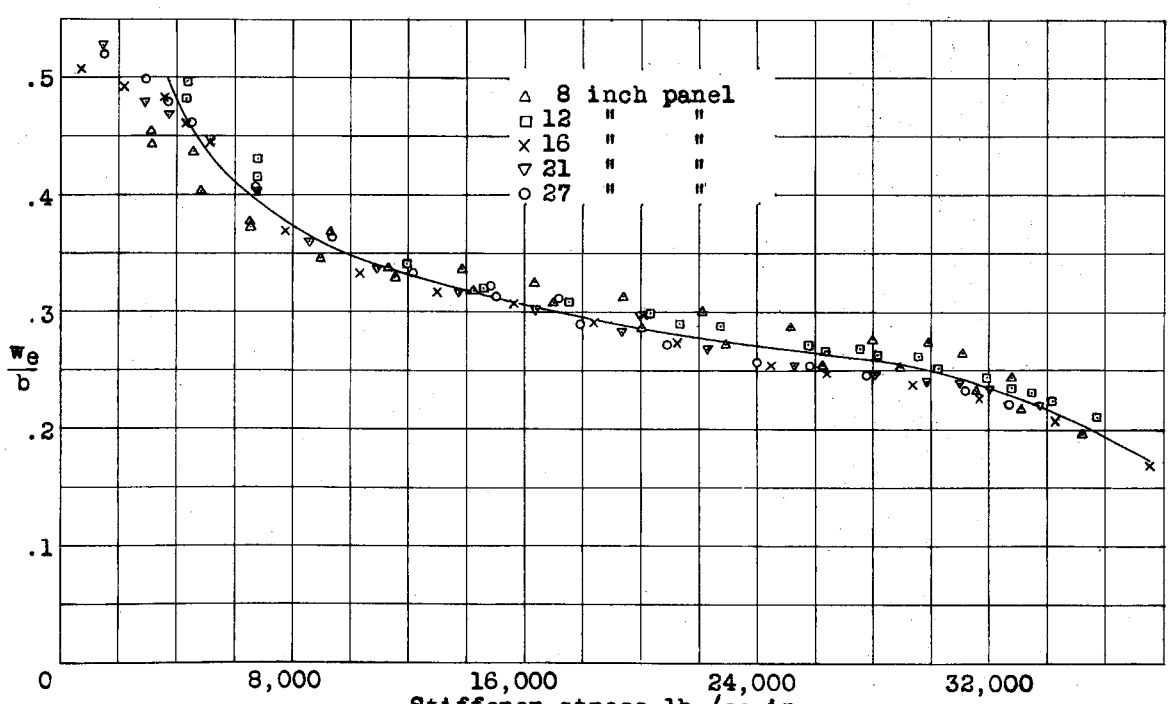

Figure 31.- Effective-width curve of three stiffener panels. 0.040"-24ST alclad skin; bulb angle 8477.

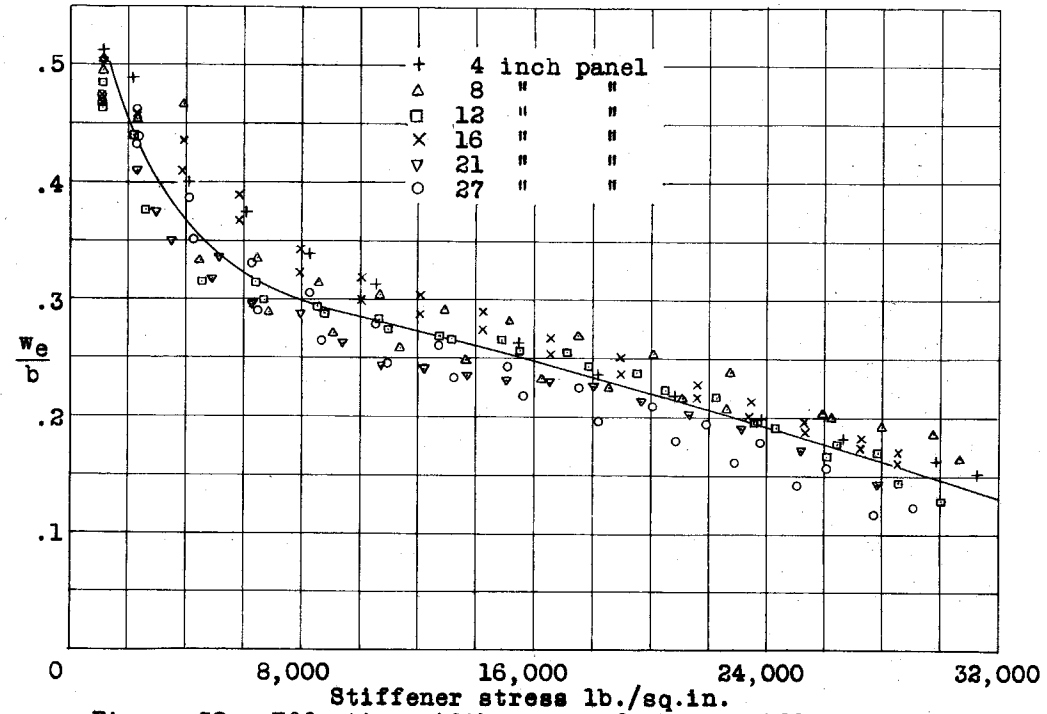

Figure 32.- Effective-width curve of three stiffener panels. 0.025"-24ST alclad skin; bulb angle 8478.

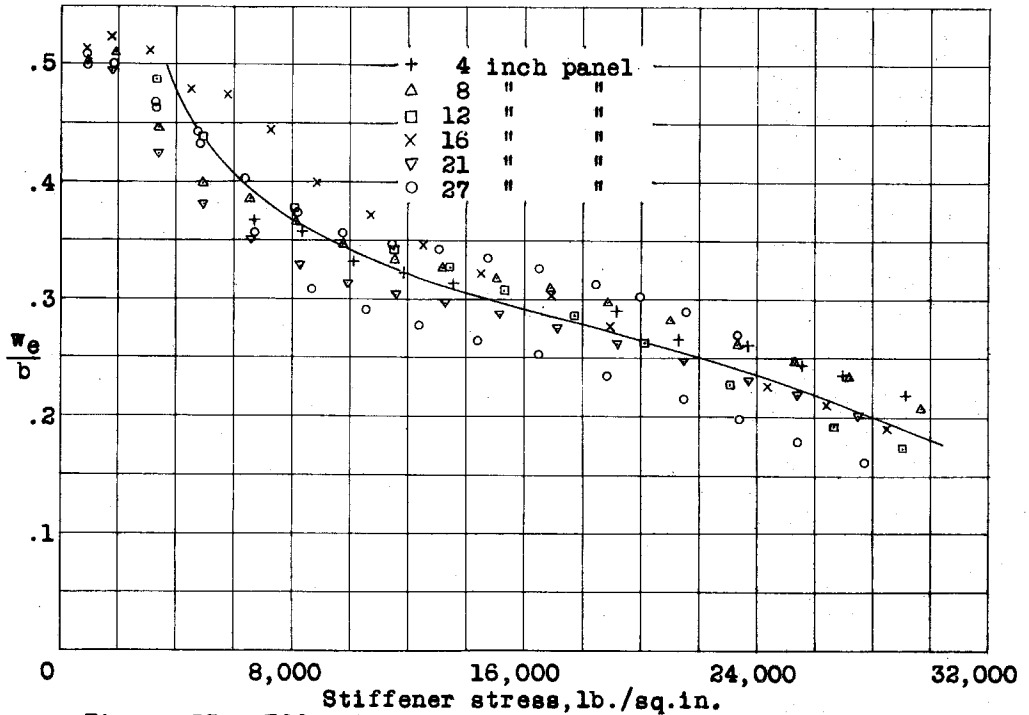

Figure 33.- Effective-width curve of three stiffener panels. 0.040"-24ST alclad skin; bulb angle 8478.

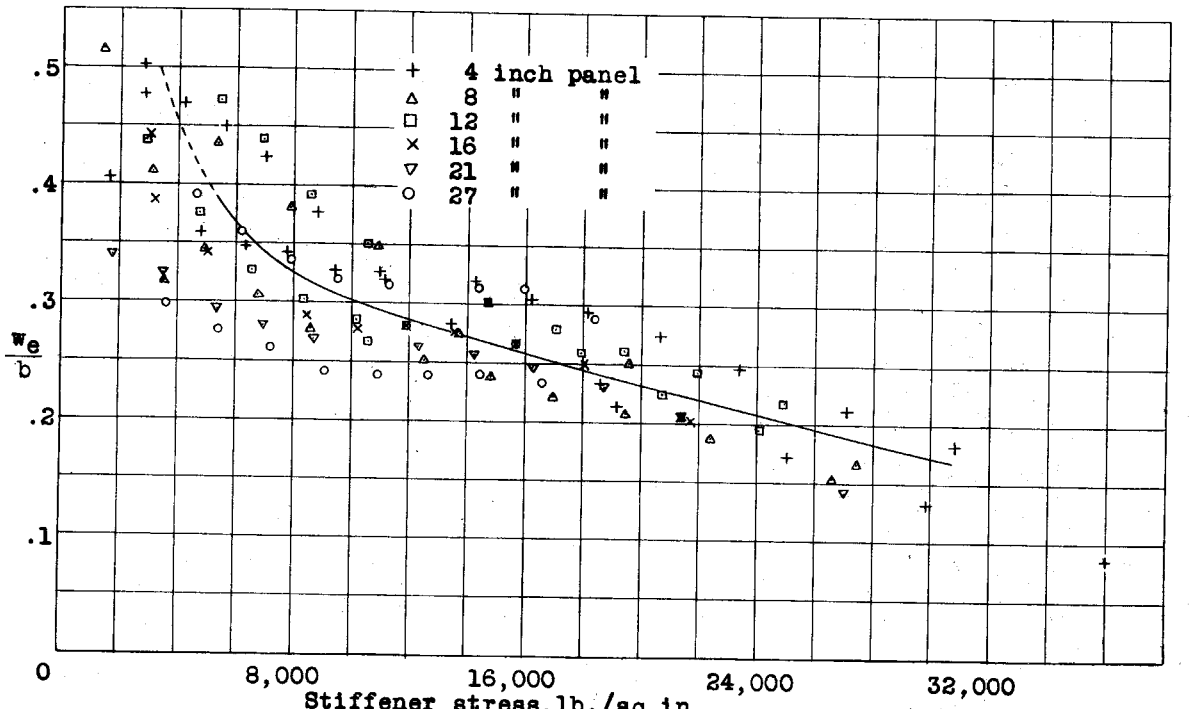

Figure 34.- Effective-width curve of two stiffener panels. 0.040"-24ST alclad skin; bulb angle 8476.

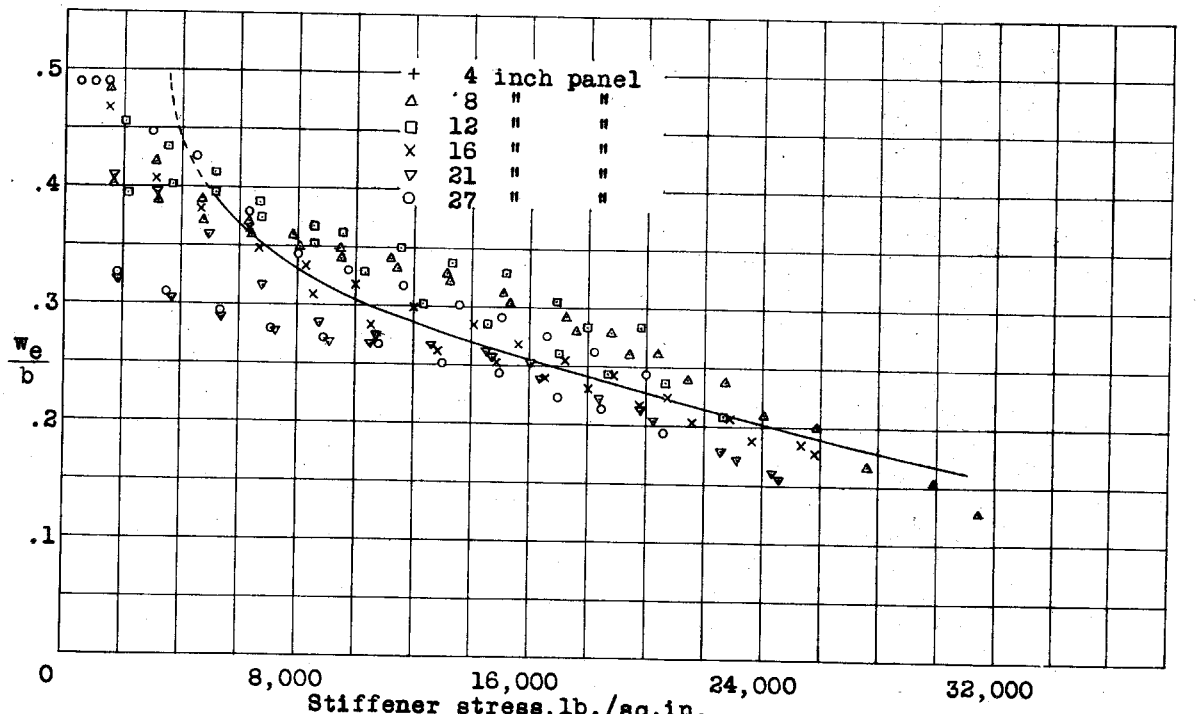

Figure 35.- Effective-width curve of three stiffener panels. 0.040"-24ST alclad skin; bulb angle 8476.

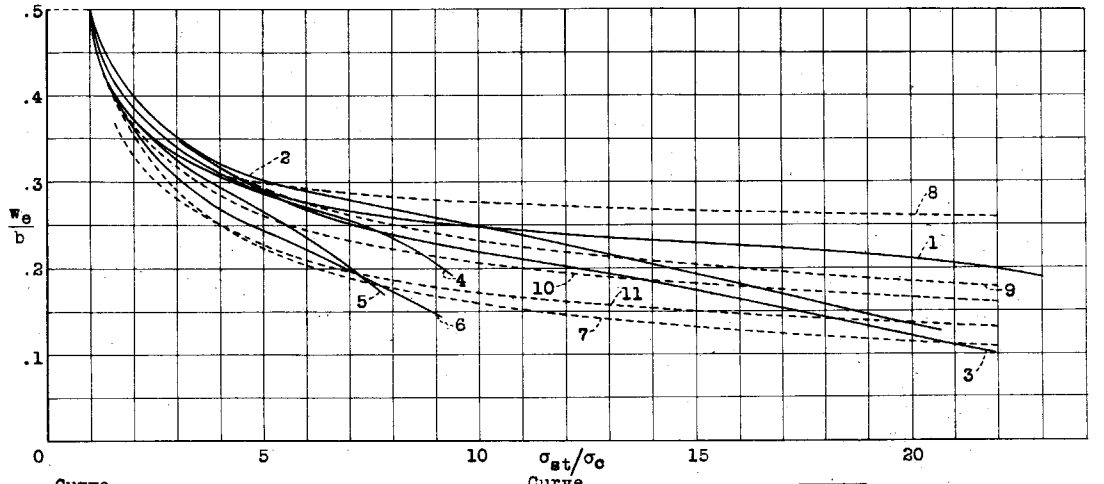

Curve					
1	Bulb angle	8477	.025"sheet		
2	"	"	8478	"	"
3	"	"	10265	"	"
4	"	"	8477	.040"	"
5	"	"	8478	"	"
6	"	"	10265	"	"

Curve		
7	von Kármán	$\frac{w_e}{b}=0.5\sqrt{\sigma_c/\sigma_{st}}$ (reference 12)
8	Sechler	$\frac{w_e}{b}=0.25\left[1+\sigma_c/\sigma_{st}\right]$ (reference 10)
9	Marguerre	$\frac{w_e}{b}=0.5\sqrt{\sigma_c/\sigma_{st}}$ (reference 11)
10	Cox	$\frac{w_e}{b}=0.5\left[0.14+0.85\sqrt{\sigma_c/\sigma_{st}}\right]$ (reference 13)
11	Cox	$\frac{w_e}{b}=0.5\left[0.09+0.80\sqrt{\sigma_c/\sigma_{st}}\right]$ (reference 13)

Figure 36.- Experimental and theoretical data on effective width variation with σ_{st}/σ_c .

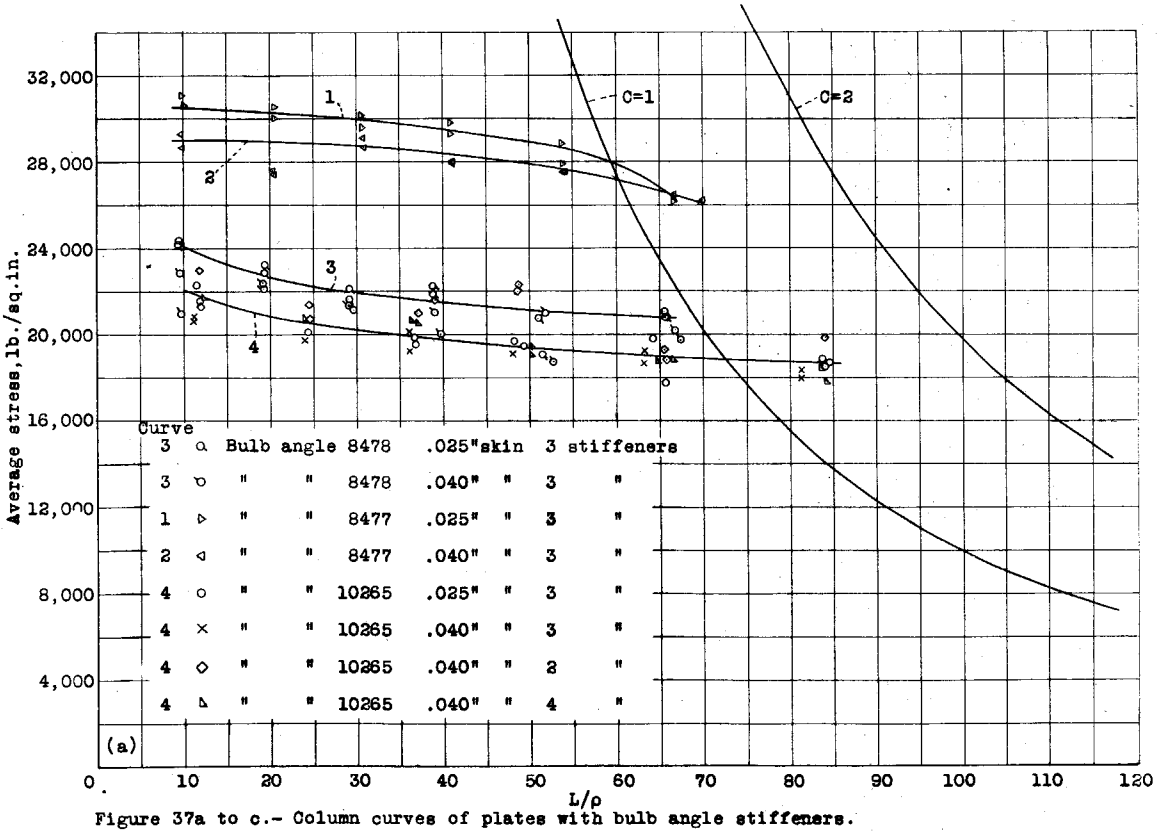

Curve							
3	○	Bulb angle	8478	.025"skin	3	stiffeners	
3	○	"	" 8478	.040"	" 3	"	
1	▷	"	" 8477	.025"	" 3	"	
2	◁	"	" 8477	.040"	" 3	"	
4	○	"	" 10265	.025"	" 3	"	
4	×	"	" 10265	.040"	" 3	"	
4	◇	"	" 10265	.040"	" 2	"	
4	△	"	" 10265	.040"	" 4	"	

Figure 37a to c.- Column curves of plates with bulb angle stiffeners.

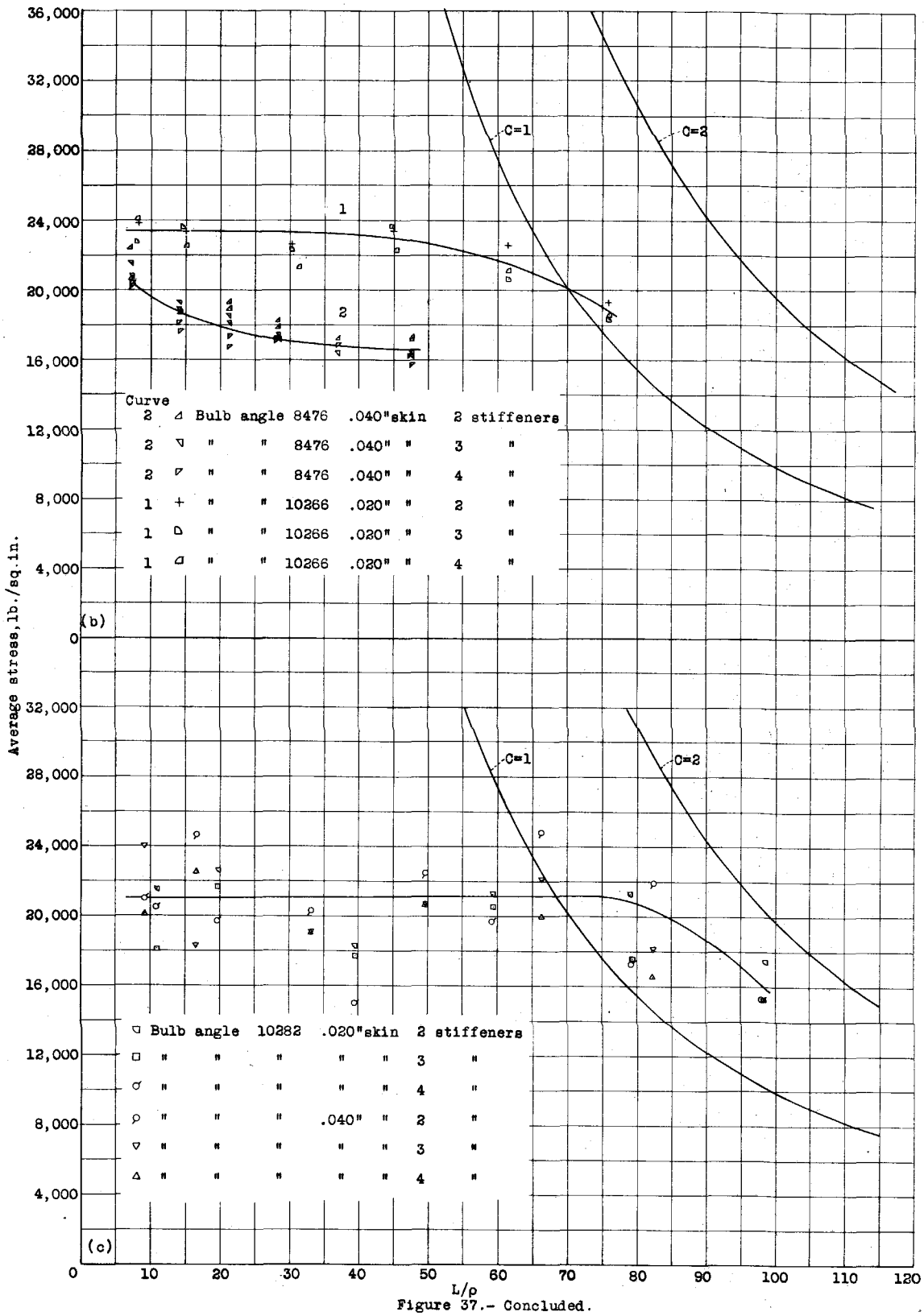

Figure 37.- Concluded.

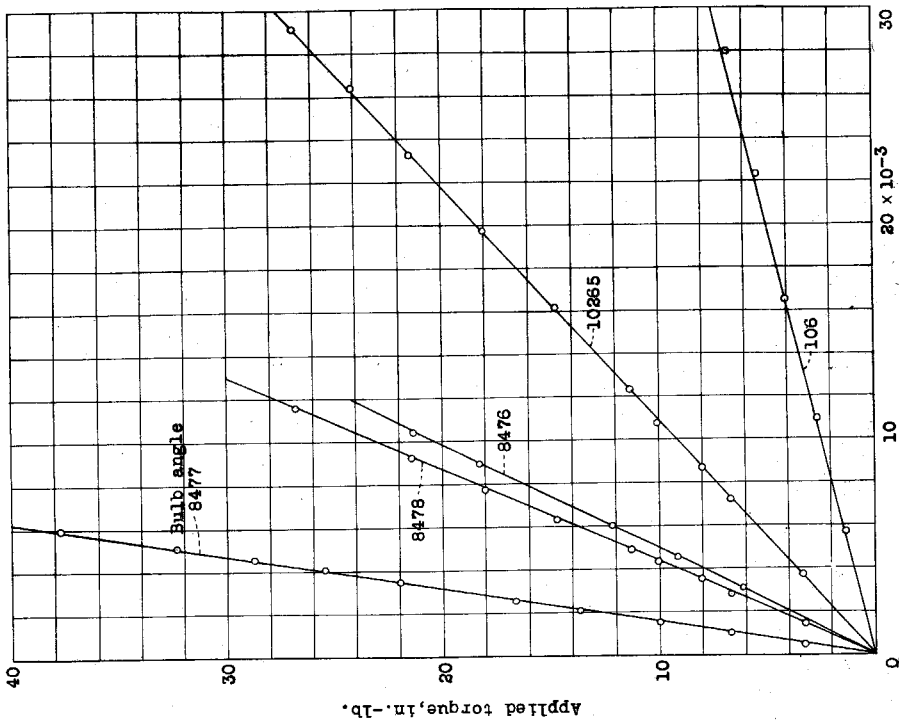

Figure 38.- Torsion tests of five stiffeners.

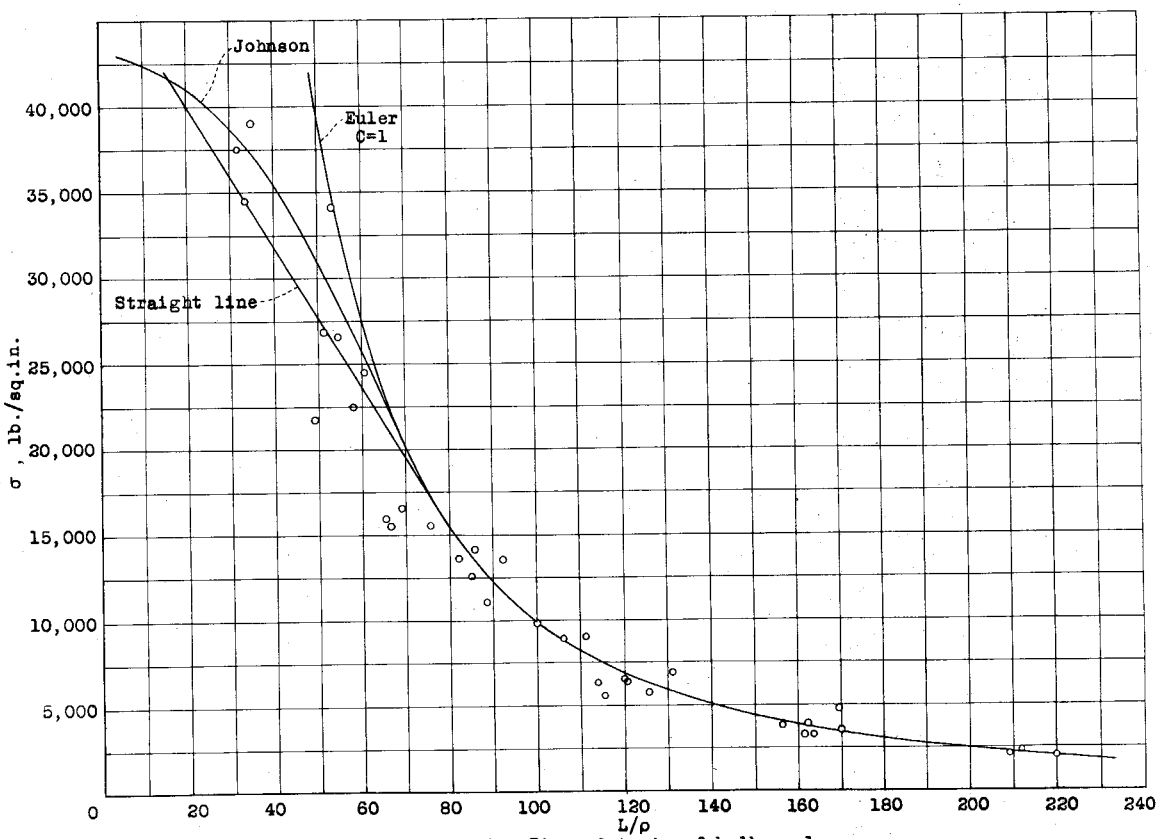

Figure 39.- Pin-end tests of bulb angles.

Straight-line formula
$\sigma = 48{,}000 - 400(L/\rho)^2$

Johnson parabolic formula
$\sigma = 43{,}000 - \frac{43{,}000(L/\rho)^2}{4\,E}$

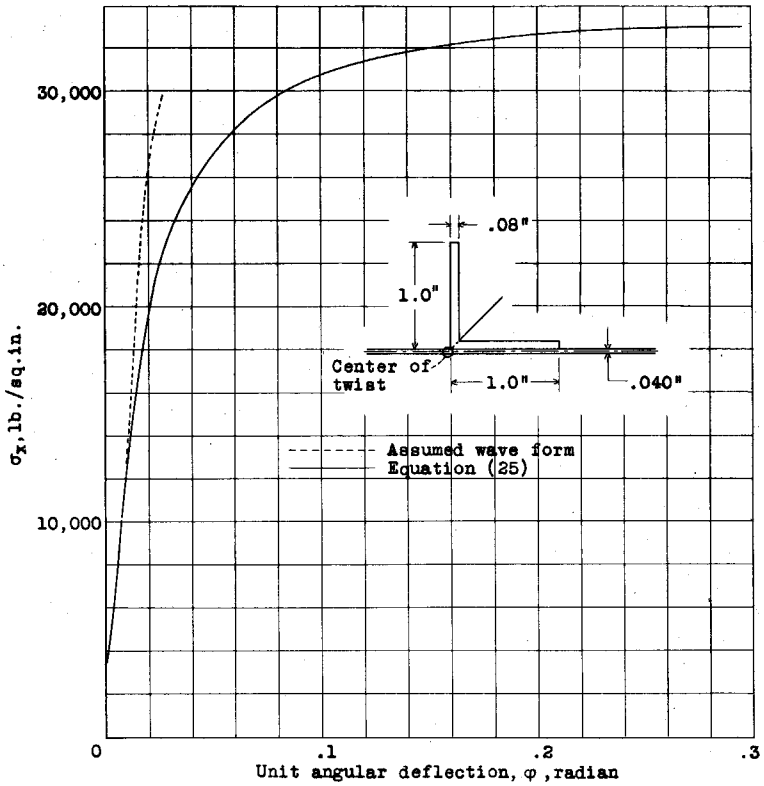

Figure 40.- Torsional deflection of the stiffener as a function of the stiffener stress.

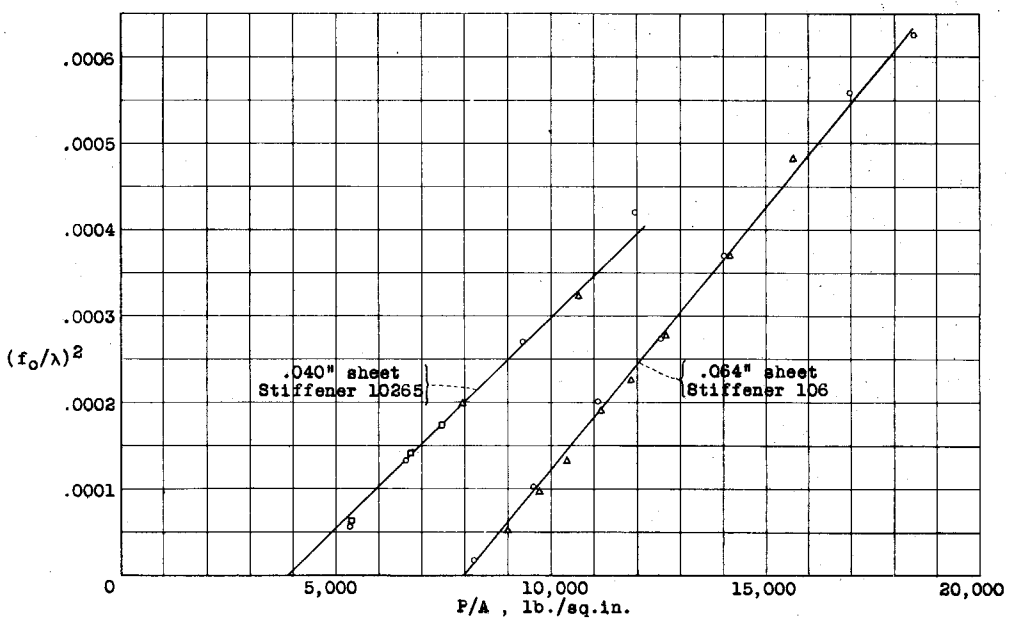

Figure 42.- Experimental curves for determining the buckling stress of the sheet.